Validation and verification of Phast CFD: a comparative analysis with Phast, KFX and tests

DNV

Date: March 2024

Reference to part of this report which may lead to misinterpretation is not permissible.

No.	Date	Reason for Issue	Prepared by	Verified by	Approved by
0	March 2024	Phast CFD	Yongfu Xu	David Alvarez Boedo Michael Harper	Trixie Secillano

Date: March 2024

Prepared by: Digital Solutions at DNV

Summary

Phast 9.0 provides users with the capability to simulate pool fires, jet fires and vapour dispersion using the Phast software and the Phast CFD capabilities within Phast (i.e. running KFX via the Phast interface) for hazard assessment. Some users may also have access to the KFX software (i.e. running cases via KFX interface directly).

This document provides validation and verification of the results produced by Phast CFD, powered by KFX, by comparing them with those from Phast and KFX. It summarises the work conducted by DNV to analyse a range of test cases for dispersions, jet fires and pool fires using Phast, Phast CFD and KFX, and to highlight any significant discrepancies in results between these tools and their underlying reasons.

The analysis reveals the following findings:

- Dispersion predictions: Predictions of dispersion for vapour releases by Phast CFD are satisfactory. However, the predictions are sensitive to surface roughness. Thus, appropriate surface roughness values are crucial for releases near the ground, rather than relying solely on the default setting in Phast. Finer grid resolution (i.e. more than 500,000 cells) will generally produce better dispersion results and is recommended if computing resources permit.
- Two-phase ammonia test cases: For the two-phase ammonia test cases, Phast CFD tends to produce under-predictions for dispersion at locations distant from the cloud centre line. While the predictions follow a similar trend as Phast, they exhibit broader scattering. However, Phast CFD does slightly overpredict arcwise maximum concentrations for all FLADIS test cases. This behaviour in Phast CFD results can be primarily attributed to the fact that Phast CFD results are predicted with fixed wind direction, which does not account for fluctuations in ambient conditions, such as wind meandering. Additionally, droplet characteristics, including droplet size distribution and spray angle, may have also contributed to the observed under-prediction and broader scattering. For scenarios with stable ambient conditions or scenarios with fixed directions, Phast CFD should give good results. However, for cases with large variations in ambient condition, Phast CFD simulations for multiple wind speeds and directions may be necessary to achieve a comprehensive dispersion result. Users with access to the KFX software can use the KFX Large Eddy Simulation (LES) model to get more accurate dispersion results, but the computing time will be significantly longer.
- Jet fire predictions: While predictions of jet fires by Phast CFD are satisfactory, potential under-predictions are observed for jet fire scenarios with large release areas, i.e. scenarios with large, expanded diameters.
- Pool fire predictions: Predictions of pool fires by Phast CFD are also satisfactory. The results are sensitive to surface roughness; therefore, appropriate surface roughness is essential, rather than relying solely on the default setting in Phast.

It is important to note that the test cases analysed in this work did not include complex geometries, as these cases can be effectively solved by simple models implemented in Phast. Phast CFD and KFX employ advanced numerical methods and algorithms to solve and analyse problems of fluid flows and excel in scenarios involving complex terrains and geometries. For cases with complex geometries or requiring detailed results, Phast CFD and KFX offer superior capabilities.

Table of contents

List of figures

List of tables

1 INTRODUCTION

In our continuous effort to advance our consequence modeling capabilities, we have incorporated computational fluid dynamics (CFD) capabilities in the Phast software to enable users to conduct comprehensive modeling of jet fires, pool fires, and dispersion scenarios. We've progressively introduced these CFD capabilities: pool fire modeling in version 8.6, jet fire modeling in version 8.7, and dispersion modeling in version 9.0, through Phast CFD. Phast CFD is powered by the KFX software, our advanced CFD simulation software for fires and dispersion. Some users may also have access to KFX (i.e. running cases via KFX interface directly). Naturally, variations in results can occur between these tools for the same case.

This document provides validation and verification of the results predicted by Phast CFD by comparing them with those from Phast and KFX. Through a series of test cases, we assess the accuracy of Phast CFD, identify any significant discrepancies, and investigate their causes. Such validation and verification are crucial to ensure our software's reliability and effectiveness in supporting critical safety decisions.

Each test case analysis begins with building a Phast case, then running it with both Phast and Phast CFD. If differences are observed, KFX, which offers more model control, is used for further investigations.

While this analysis currently covers only a selection of test cases, not all Phast test cases are included in this work and ongoing updates to this document will include additional scenarios as more results become available.

2 METHODOLOGY

2.1 Terminology

Four types of results are compared in this document:

- Test results, also refer to as observed data, were obtained through experiments and tests and are used to validate model predictions.
- Phast results were predictions generated by models implemented within Phast.
- Phast CFD results were predictions produced by running KFX through the Phast interface. Assumptions have been made by Phast CFD to enable accurate CFD results with minimal efforts. It is important to note that users have limited control over the modelling and the default model settings may lead to less accurate results for some cases.
- KFX results were predictions obtained using the KFX graphical user interface (GUI) of the KFX software. While most KFX runs in this work started with JSON files generated by Phast as inputs, some changes were made manually based on complexity of the geometry and release scenarios. These changes include grid distribution, parameter settings or additional outputs.

2.2 The approach

The majority of the cases analysed in this work are test cases of the Phast models. The following steps were taken for each case to generate results for comparison:

1. **Phast results**. Phast results were primarily obtained from existing study files of the test cases, with a few cases generated to test specific scenarios.
2. **Phast CFD results**. For dispersion cases, Phast CFD, powered by KFX, was executed from Phast via CFD dispersion cases created within Phast. Jet fire and pool fire cases were run from the Phast scenarios directly.
3. **KFX results.** For cases needing more control over the model, such as grid, parameter settings or additional outputs, KFX was run using JSON files created by Phast as inputs.
4. **Comparing results.** Results from Phast CFD are compared with Phast predictions and test results if available. For dispersion scenarios, the comparative analysis includes contours of specified concentrations and concentrations at specific points or along arcs. In cases of jet fires and pool fires, the focus is on comparing radiation levels at measurement points. In instances where significant discrepancies are noted, KFX results are applied to understand the differences.

3 DISPERSION RESULTS

3.1 Vapour release of methane

3.1.1 The base case of sensitivity analysis

This is a simple test specially created to assess sensitivity of Phast CFD predictions to grid distributions and parameter settings. The results are only compared against Phast predictions. Table 1 below lists the release and ambient conditions of the case. High jet velocity significantly increases CFD running time. In this sensitivity analysis, the vessel pressure was intentionally set low to ensure a reasonable CFD running time for a large number of cases. The discharge velocity of this methane case is 165 m/s, which may be lower than in many release scenarios; however, the findings should still be applicable to a wide range of vapor release situations.

Table 1 Release and ambient conditions of the base case

	Value
Material	methane
Vessel pressure (barg)	0.1
Vessel temperature (degC)	10
Vessel inventory (kg)	10000
Release height (m)	1
Hole size (mm)	100
Ambient air temperature (degC)	9.85
Ambient air pressure (bar)	1
Ambient humidity (%)	70
Wind Speed (m/s)	5
Pasquill stability	D
Averaging time (s)	18.75 (Phast results)
Surface roughness (mm)	5 183.15 (Phast default)

3.1.2 Result of the base case

- Differences are observed between dispersion results by Phast and Phast CFD for the base case at default setting for surface roughness in Phast, i.e. 183.156mm, as shown in Figure 1 & Figure 2. The differences can be attributed to several factors:
  - Phast CFD imposes a limit on surface roughness that may lead to a smaller roughness value being used in simulations for cases with large roughness, such as the default roughness value in Phast. When surface roughness is larger than the height of the control volumes used in a CFD simulation, it implies that there is geometry considered by Phast CFD, so that downwind obstructions (i.e. 3D geometry or terrain data) resemble the surface roughness.
  - Phast CFD directly simulates the ground effects on vapour dispersions.
- Dispersion results from Phast CFD are shown to be sensitive to grid resolution, release height and surface roughness as shown in Figure 3, Figure 4 & Figure 5, respectively.
- Finer grid resolution (i.e. more than 500,000 cells) will generally produce better dispersion results and is recommended if computing resources permit.

- Surface roughness has a large impact on dispersion results for releases near to the ground. So, it is important to select appropriate surface roughness for dispersion simulations.
- Comparison of the effect distances predicted by Phast and Phast CFD is presented in Figure 6. Large differences are revealed between Phast & Phast CFD predictions for releases near to the ground. Phast CFD gives more conservative predictions of the effect distance for releases near to the ground.

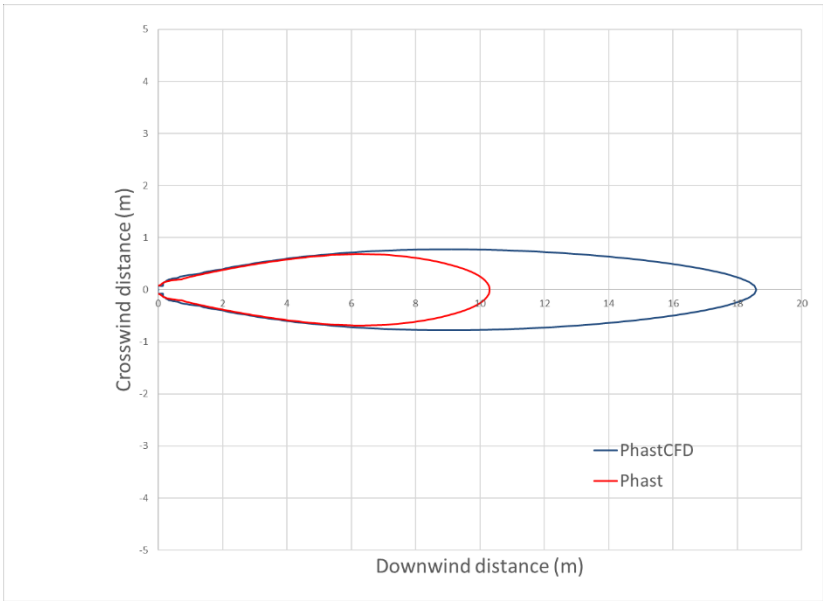

Figure 1 Footprint contours of 0.5LFL (25000ppm) at release height of the base case（default settings on parameters）

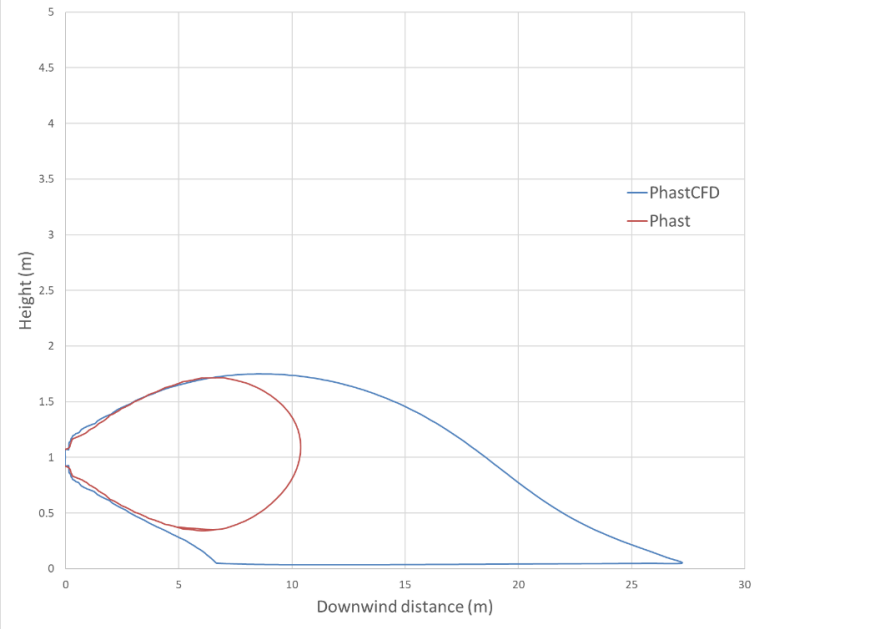

Figure 2 Sideview contours of 0.5LFL (25000ppm) crossing the release point of the base case (default settings on other parameters)

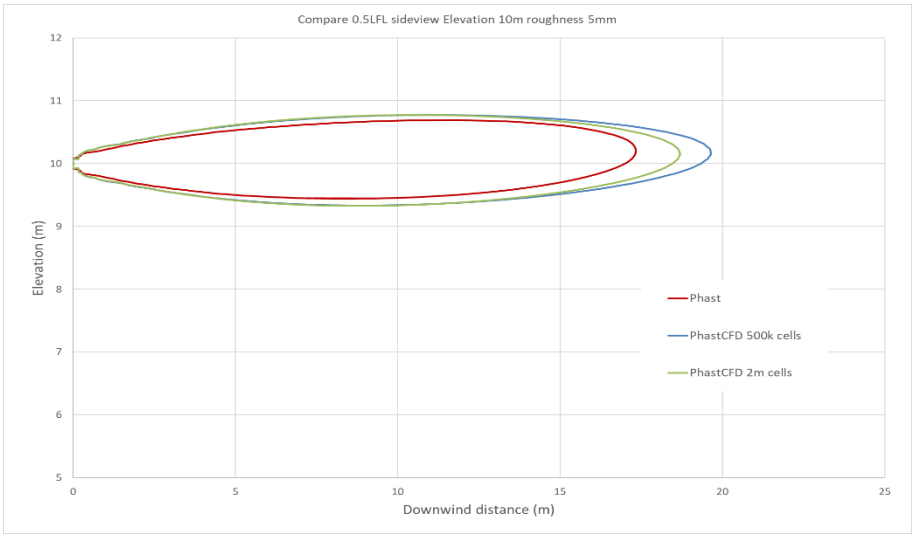

Figure 3 Effect of grid sensitivity on side views of 0.5LFL of Phast CFD predictions

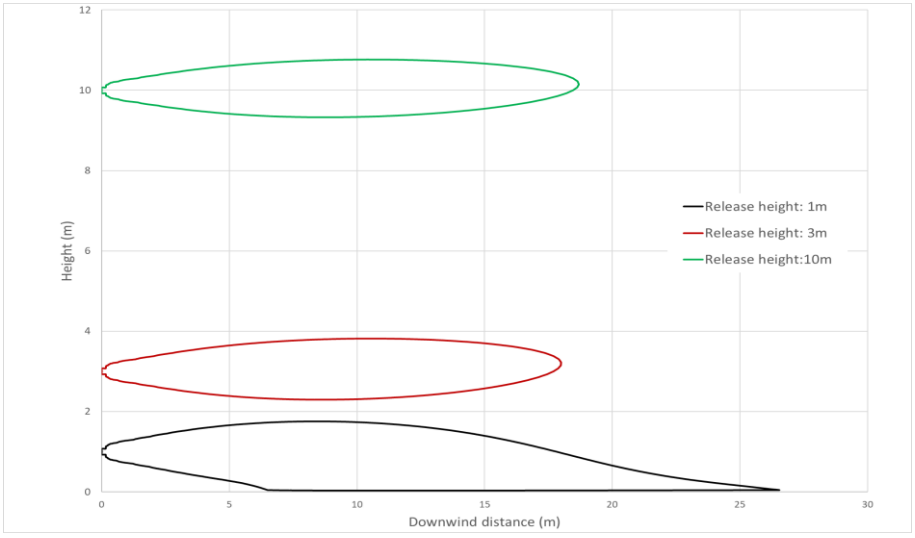

Figure 4 Effect of release height on side views of 0.5LFL of Phast CFD predictions (2 million cells, 5mm surface roughness)

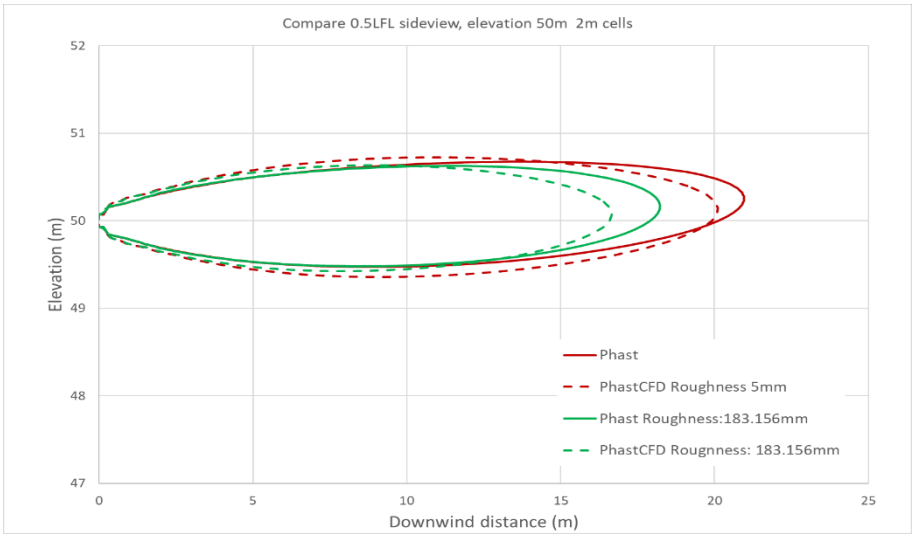

Figure 5 Effect of surface roughness on side views of 0.5LFL of Phast CFD predictions (2 million cells, release height at 50m)

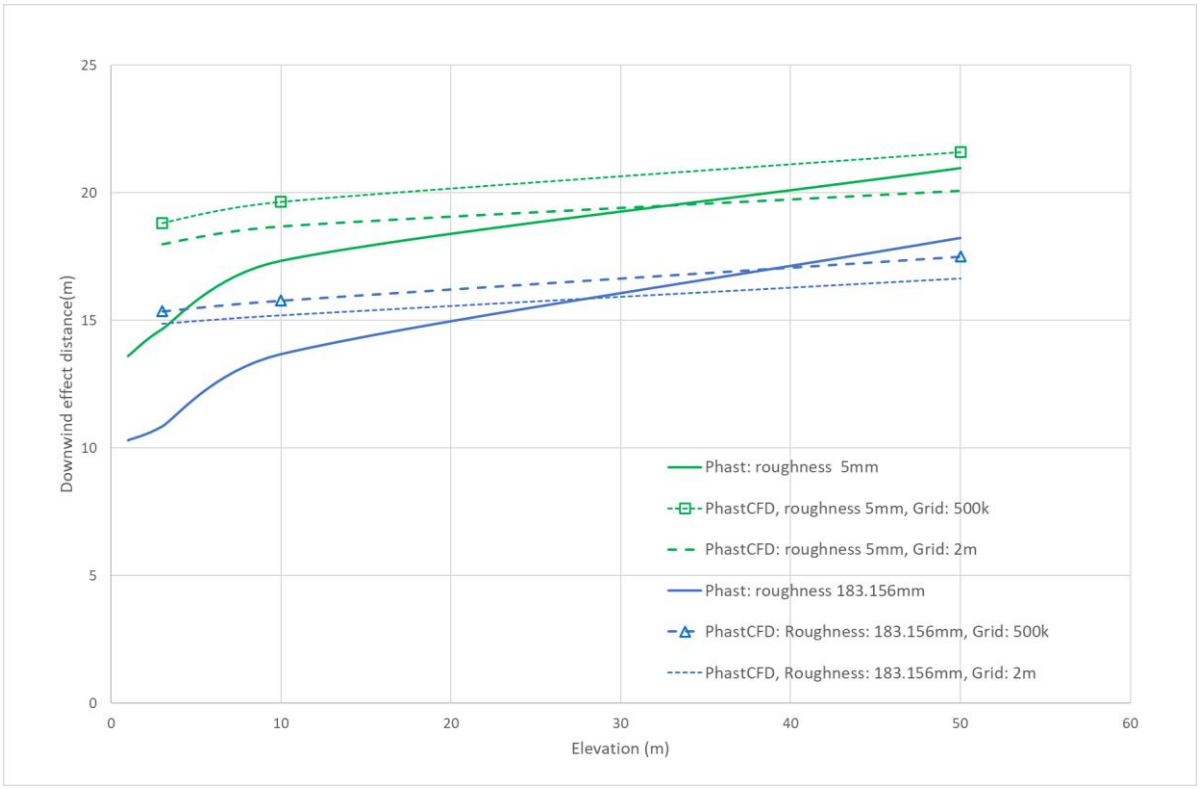

Figure 6 Comparing effect distances predicted by Phast and Phast CFD

3.2 Horizontal vapour releases of hydrogen

3.2.1 The test case

The Shell HSL tests (Roberts, 2006) were used to validate dispersion results of UDM (Unified Dispersion Model) in Phast. Measurements of arc-wide max concentrations were used in the validation. Table 2 below shows input data of the Shell HSL09 test case for Phast and Phast CFD simulations.

Table 2 Release and ambient conditions of Shell HSL09

	Shell HSL09
Material	Hydrogen
Mass flowrate (kg/s)	0.0728
Release temperature (deg C)	-130
Release velocity (m/s)	2036
Release height (m)	1.5
Hole size (mm)	3
Ambient air temperature (deg C)	13.5
Ambient air pressure (bar)	1
Ambient humidity (%)	70
Wind Speed (m/s)	3
Pasquill stability	D
Averaging time (s)	18.75 (Phast results)
Surface roughness (mm)	10

3.2.2 Results and Observations

- The contours of LFL & 0.5LFL predicted by Phast CFD for this case do not touch the ground (as shown in Figure 7) and are similar to the Phast predictions (as shown in Figure 8).
- Phast CFD predicts longer 0.25LFL contours compared to Phast predictions. The predicted 0.25LFL contour extends to the downwind boundary of the computational domain (as shown in Figure 7), which suggests that a larger computational domain is necessary for Phast CFD if 0.25LFL concentration is of concern.
- Predictions from both Phast & Phast CFD show good agreement with measurements of max arc-wide concentrations, as illustrated in Figure 9 & Figure 10. The geometrical mean bias, MG, and geometric variance, VG, are two statistical values in commonly used to assess quality of datasets. These measurements are all within 11m from the release point at the release height and so fall within the contour of predicted 0.5LFL concentration. The relatively stable ambient conditions may have led to the max arc-wide concentrations occurring near to cloud centre line, potentially contributing to the good agreement between the predictions and measurements.

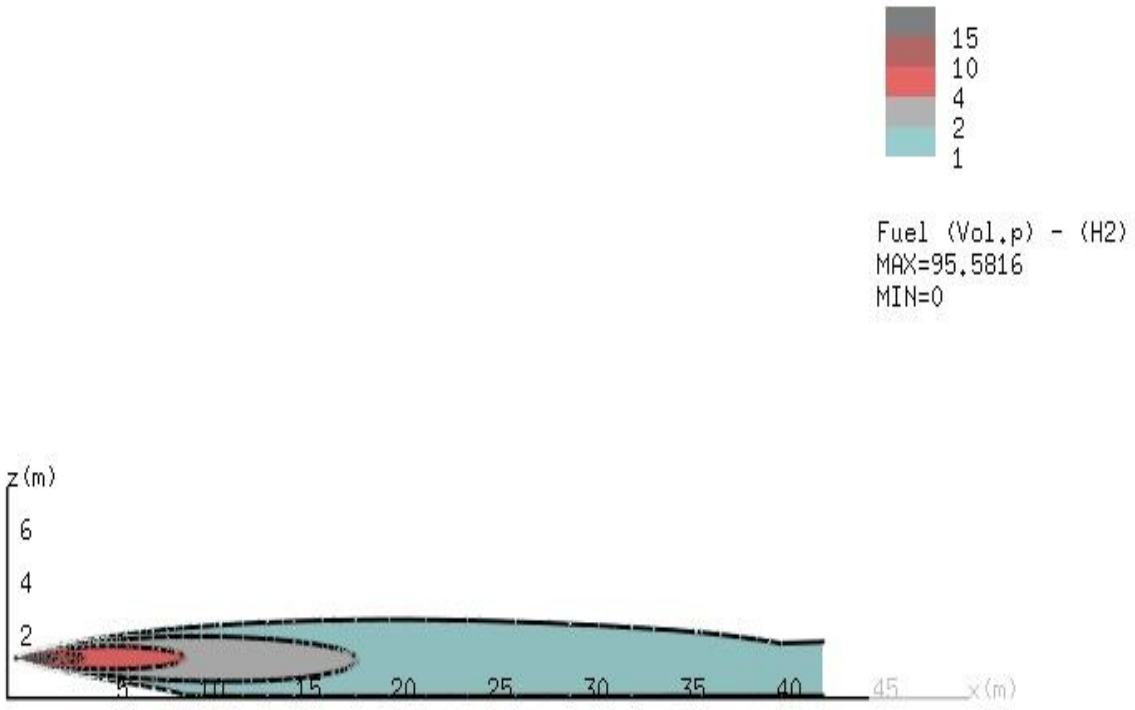

Figure 7 Phast CFD predictions of cloud side view (grey contour corresponds to 0.5LFL concentration)

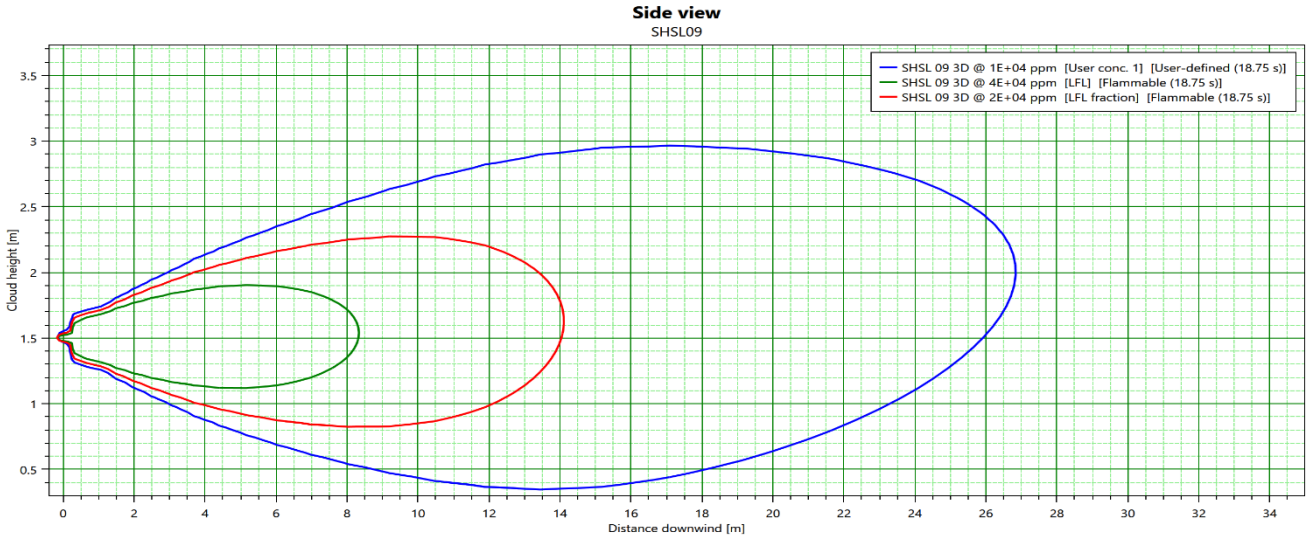

Figure 8 Phast predictions of cloud side views (red contour corresponds to 0.5LFL concentration)

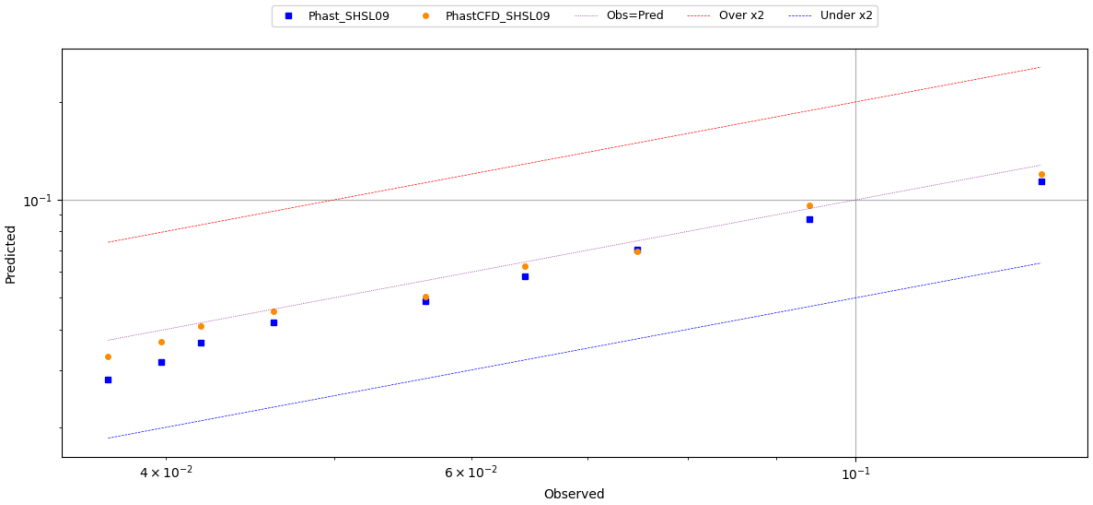

Figure 9 Comparing measured arc-wise max concentrations against predictions by Phast CFD and Phast

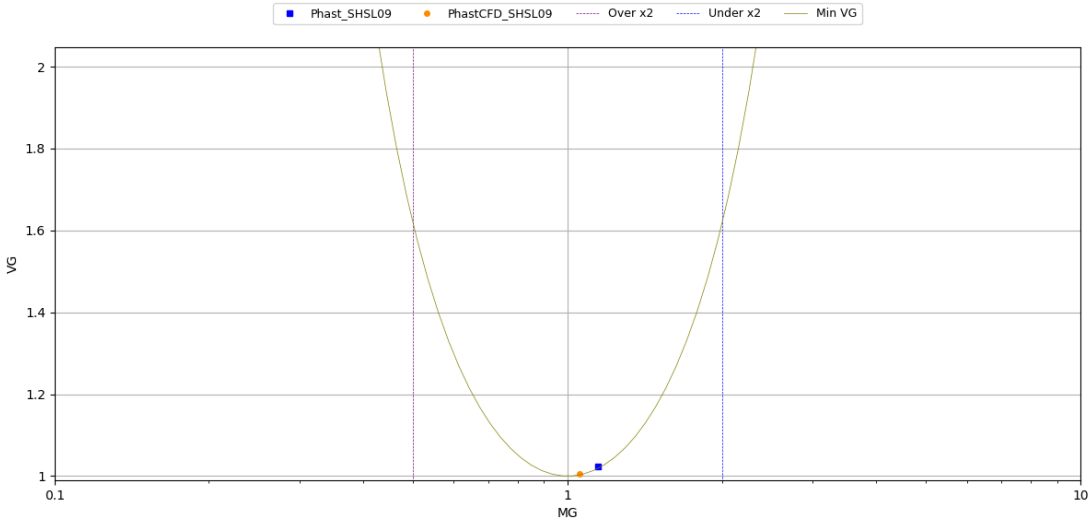

Figure 10 Statistical assessment of measured arc-wise max concentrations against predictions by Phast CFD and Phast

3.3 Vertical releases of natural gas and hydrogen

DNV consultants have performed CFD simulations of vertical venting of natural gas and hydrogen using FLACS. The work focused on determining the effect ranges of hydrogen and natural gas releases (i.e. the downwind extents and heights of the cloud) at specified concentrations, particularly the 0.5LFL concentration. While details of these simulations are confidential, the following observations have been made:

- Both Phast CFD and FLACS generate very similar predictions in trends and magnitudes of the effect ranges for the simulated scenarios of hydrogen and natural gas releases.
- Phast produces results that are comparable to Phast CFD and FLACS in terms of the heights of 0.5LFL contours for both natural gas and hydrogen release scenarios. However, Phast results tend to be more conservative in predicting the extent of 0.5LFL contours at high wind speeds and less conservative at low wind speeds.

3.4 Two-phase release of ammonia

3.4.1 Test cases

FLADIS (Nielsen, 1996) is a project designed to investigate dispersion of ammonia aerosols. Liquefied ammonia was released under pressure through a nozzle positioned at a height of 1.5m. The experiments, characterised by low release rates, were aimed at investigating the far-field passive effects. Ammonia was released in two phases, but no liquid pool was observed during the tests. Table 3 below shows the input data for Phast & Phast CFD simulations. Figure 11 shows the locations where concentrations were measured in the test. Most of the concentration sensors were arranged on three arcs at distances of 20m, 70m and 238m. Further details of the tests can be found in the Phast validation document for the Unified Dispersion Model (DNV, Validation: Unified Dispersion Model, 2023).

Table 3 Release and ambient conditions for the FLADIS experiments

Series	**FLADIS**
Substance	Ammonia
Release type	Continuous
Release height, m	1.5
Jet type	Horizontal
Dispersing surface	Land
Surface roughness length, m	0.04
Solar flux, W/m^2	500

FLADIS 9	**FLADIS 16**	**FLADIS 24**	
0.4	0.27	0.46	Release rate, kg/s
900	1140	600	Duration, s
D	E	C	Stabiltiy class
5.6	4.4	5.03	Wind speed at reference height, m/s
288.7	290	291	Ambient temp., K
0.86	0.62	0.536	Relative humidity fraction
102000	102000	101300	Atmospheric pressure, Pa
288.7	290	291	Dispersing surface temp., K
0.84	0.83	0.83	Discharge liquid mass fraction
65.17	67.85	55.87	Release velocity, m/s
10	10	10	Reference height for wind speed, m
10	10	10	Reference height. for air temp, m
0.0823	0.0772	0.114	Drop diameter, mm
600	600	400	Averaging time (s)

1) These data were provided as part of the SMEDIS project
2) For FLADIS16 the stability class was given as being D/E. This option is not available within the UDM, hence stability class E was taken as a conservative option.
3) The reference height for temperature was set equal to the reference height for windspeed.
4) The surface temperature was set to the temperature at the reference height.

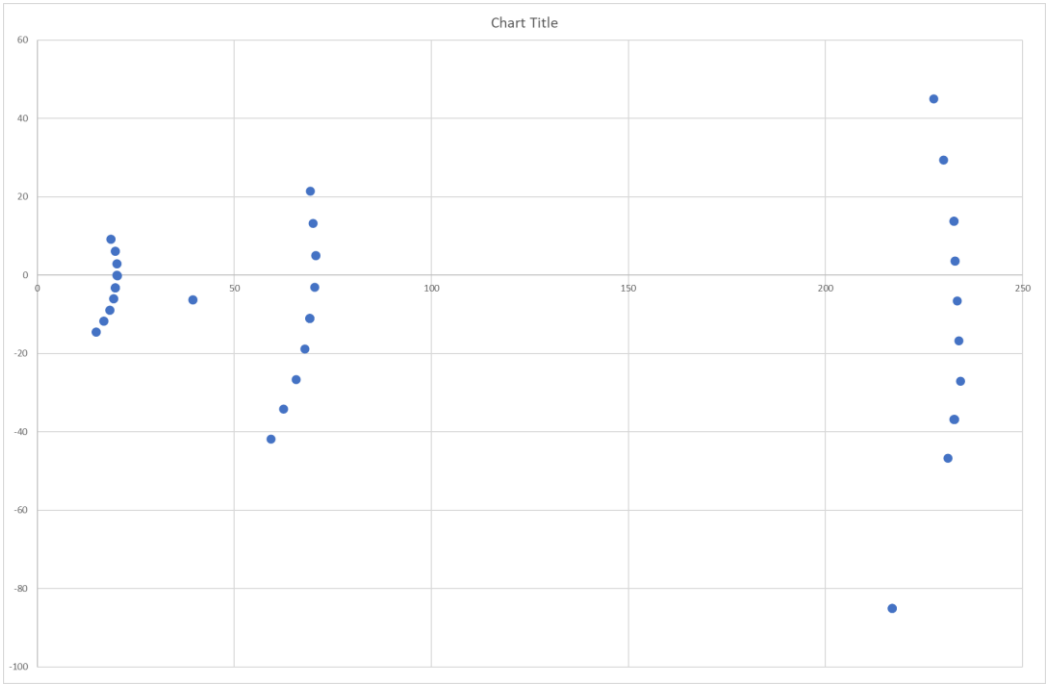

Figure 11 Locations of concentration sensors in the FLADIS experiments

3.4.2 Sensitivity study using the FLADIS09 test case

- Figure 12 & Figure 13 compare the contours of ERPG3 concentration of ammonia, i.e. 750ppm, predicted by Phast and Phast CFD. Phast predictions appear to be more conservative in this case.
- Figure 14 compares dispersion results with varied grid resolutions and user-defined domain sizes. While the default number of grid cells (500,000) produces similar results to 2 million cells, the default domain size based on Phast results seems large, particularly in the vertical direction. A reduced domain size via user-defined domain setting has resulted in slightly improved predictions
- Figure 15 shows the sensitivity of predicted concentrations to spray characteristics for liquid ammonia in the releases. Three results are as follows:
  - Default specification: uniform droplet size and a spray angle of 30 degrees
  - 60 deg: uniform droplet size and a spray angle of 60 degrees
  - DropletDist: a log-normal distribution of droplet sizes and a spray angle of 30 degrees

  Spray characteristics do have some impacts on dispersion results. The release with an increased spray angle of 60 degrees yields marginally better results than the other two spray specifications in this test case.
- Based on this sensitivity analysis, the results presented below for the FLADIS experiments are modelled with the following settings: reduced domain size, 2 million grid cells and default spray specification. Domain size and cell number can be adjusted in Phast CFD via the *CFD grid parameters*.

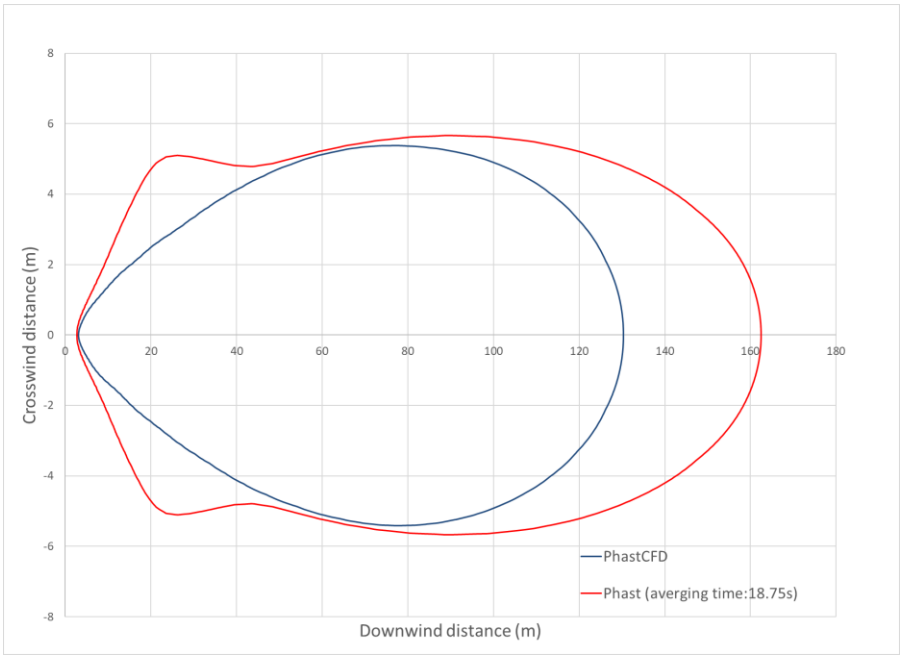

Figure 12 Concentration footprint of 750ppm (ERPG3) at the release height

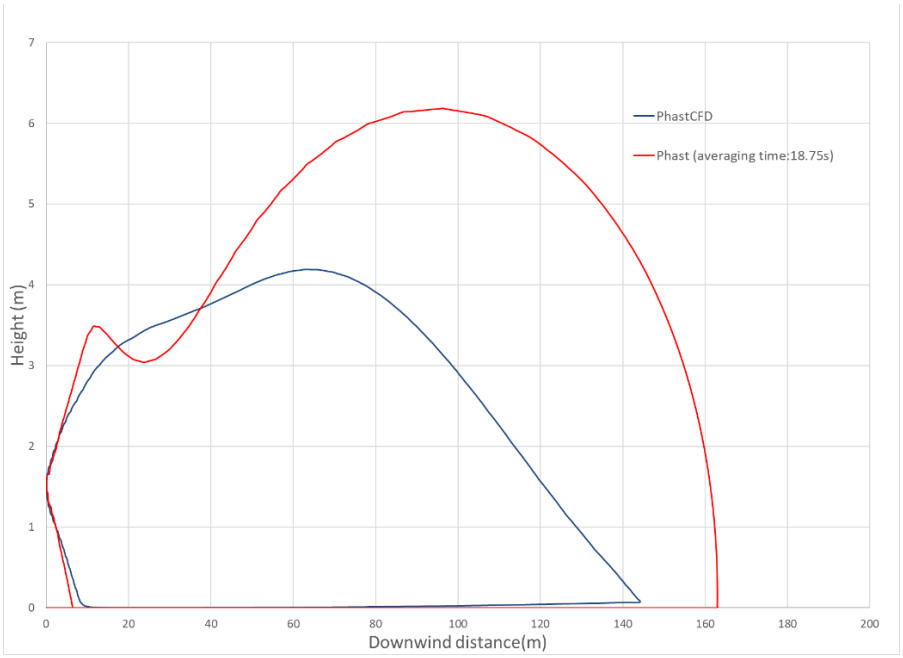

Figure 13 Concentration sideview of 750ppm (ERPG3) crossing the release point

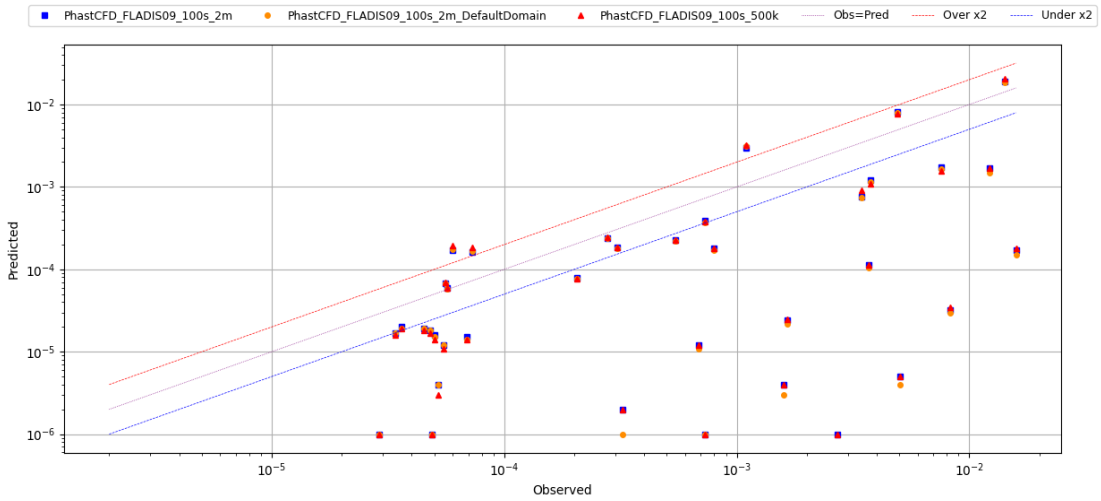

Figure 14 Results sensitivity to grid and domain size (Blue: 2 million grid cells and user defined domain size; Orange: 2 million grid cells and default domain size; Red: 500,000 grid cells and used defined domain size)

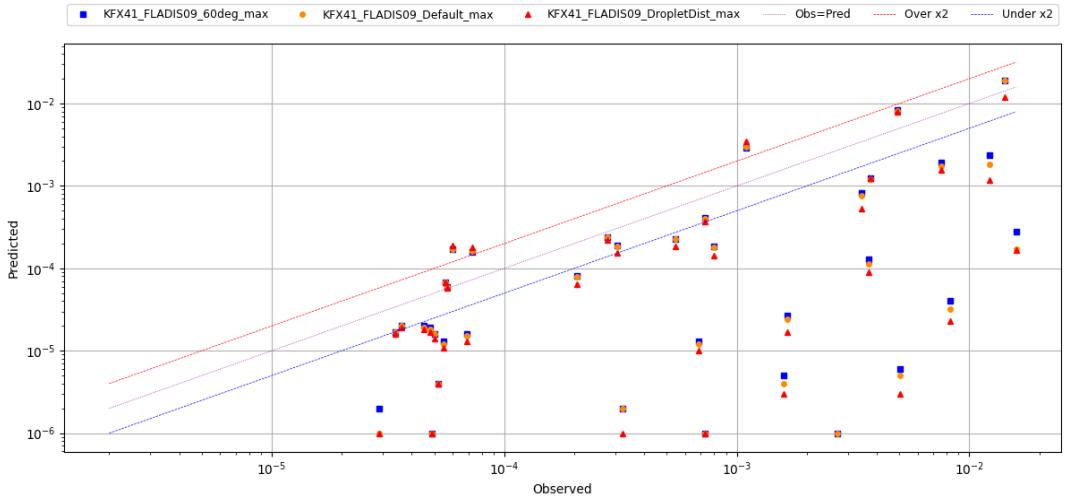

Figure 15 Results sensitivity to spray specification of the FLADIS09 test case (Blue: uniform droplet size and a spray angle of 60 degrees; Orange: uniform droplet size and default spray angle of 30 degrees; Red: a log-normal distribution of droplets and default spray angle of 30 degrees)

3.4.3 Results and Observations of the FLADIS test cases

- Phast CFD predictions for the three FLADIS test cases are shown in Figure 16, Figure 17 and Figure 18. The predictions exhibit deviations from test measurements, with broader scattering compared to Phast predictions.
- Figure 19 illustrates contours of ERPG2 & ERPG3 concentrations predicted by Phast CFD, along with the locations of sensors exhibiting significant under-predictions. The majority of the under-predictions occur outside the ERPG2 contours. The under-predictions can be primarily attributed to the fact that Phast CFD results are calculated for a fixed wind direction and do not account for fluctuation in ambient conditions, such as wind meandering. Consequently, under-predictions occur at locations far from the cloud centre line (as shown in Figure 19), owing to wind meandering's propensity to induce wider dispersion compared to a fixed wind direction. Wind meandering is addressed in Phast by applying an averaging time of 600s for ammonia. Additionally, droplet characteristics, including droplet size distribution and spray angle, may have also contributed to the observed under-prediction and broader scattering.
- To counter the influence of wind meander, a method commonly applied to evaluate dispersion predictions involves comparing arcwise maximum concentrations as used in UDM validation (DNV, Validation: Unified Dispersion Model, 2023). Figure 20 presents a comparison of arcwise maximum concentrations for the FLADIS test cases. Phast CFD tends to produce a bit overpredictions with results near top of the factor-of-two lines. Statistical MG/VG of the arcwise maximum concentrations of Phast CFD predictions are shown in Figure 21. Notably, FLADIS09 & 24 fall just outside the vertical dotted lines and confirm slight overpredictions as illustrated in Figure 20. This slight overpredictions of arcwise maximum concentration suggests that the under-predictions shown in Figure 19 are primarily due to fluctuations in ambient conditions.
- The Large Eddy Simulation (LES) model in KFX solves the largest eddies in a turbulent flow by a Navier-Stokes solver, and then models the smaller eddies by an eddy viscosity, and therefore yields more realistic results for gas dispersion and fires. However, this model is only available in KFX (i.e. not via Phast CFD) and requires significantly more computing power. The LES model in KFX was applied here to investigate the under-predictions observed in Phast CFD predictions and the results are shown in Figure 22 for the FLADIS24 test case. Even though the simulation has been stopped a bit too soon due to significant computing time, the KFX LES model does give improved predictions at some locations. The Large Eddy Simulation (LES) model may present an alternative for users with access to KFX to get more accurate dispersion results.
- For scenarios with stable ambient conditions or QRA scenarios with fixed directions, Phast CFD should give good dispersion results. However, for cases with large variations in ambient condition, Phast CFD simulations with fixed directions may significantly under-predict off-centreline concentrations. Hence Phast CFD simulations for multiple wind speeds and directions may be necessary to achieve a comprehensive dispersion result of a case. Users with access to the KFX software can use the KFX Large Eddy Simulation (LES) model to get more accurate dispersion results, but the computing time will be significantly longer.

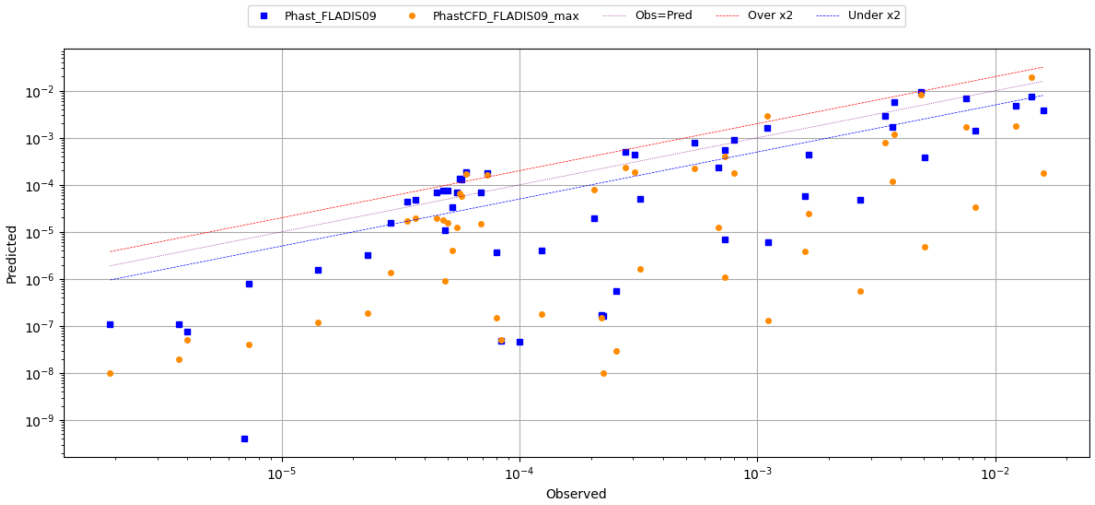

Figure 16 Comparing predictions by Phast CFD, Phast and measurements for the FLADIS09 test case (Blue: maximum concentrations predicted by Phast; Orange: maximum concentrations predicted by Phast CFD)

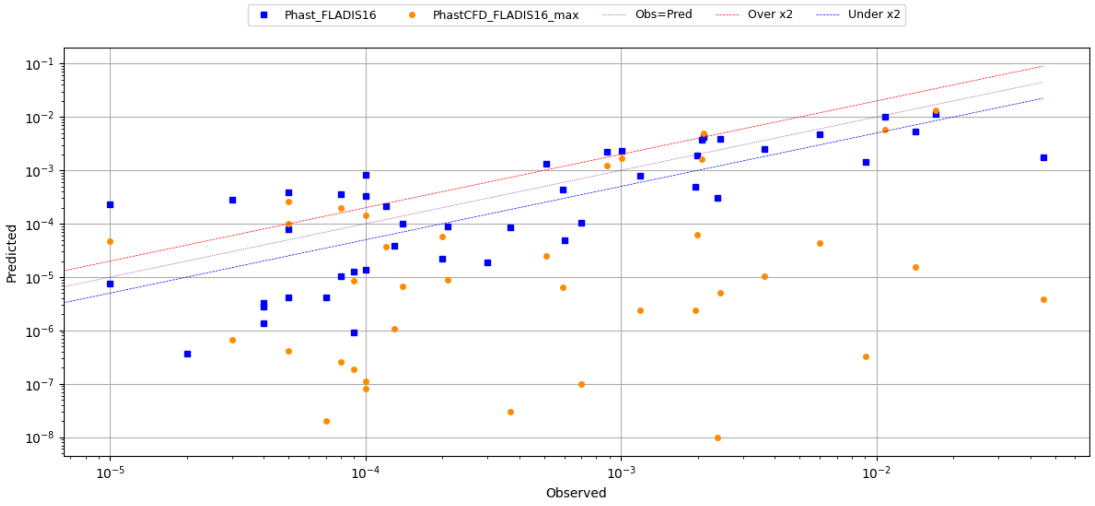

Figure 17 Comparing predictions by Phast CFD, Phast and measurements for the FLADIS16 test case (Blue: maximum concentrations predicted by Phast; Orange: maximum concentrations predicted by Phast CFD)

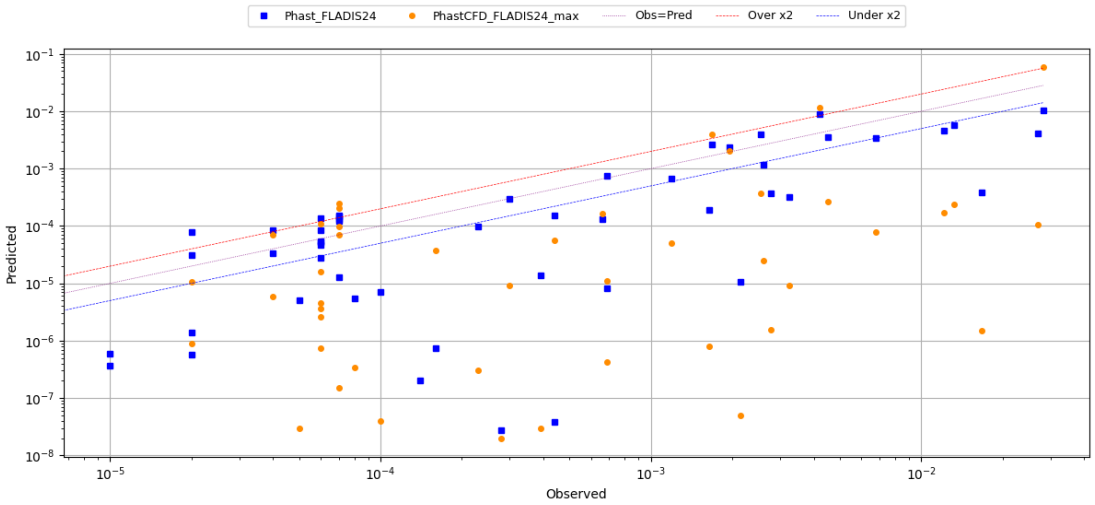

Figure 18 Comparing predictions by Phast CFD, Phast and measurements for the FLADIS24 test case (Blue: maximum concentrations predicted by Phast; Orange: maximum concentrations predicted by Phast CFD)

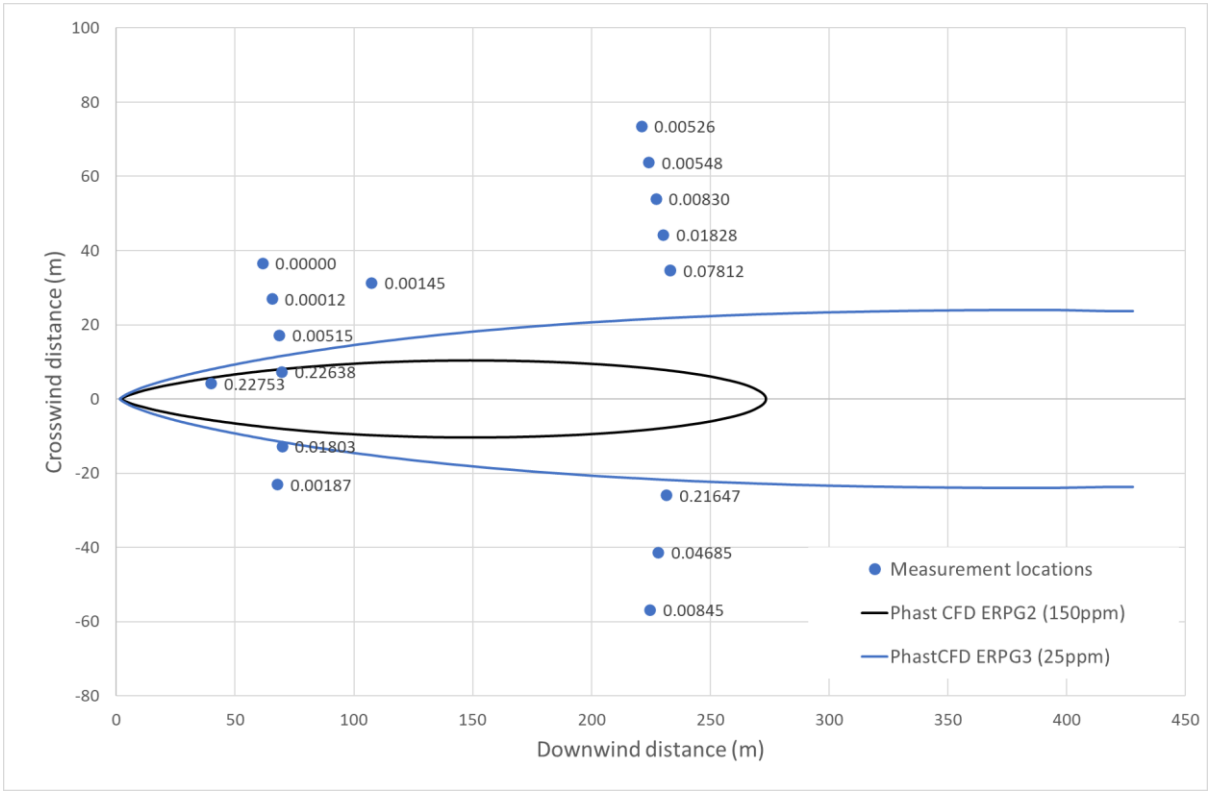

Figure 19 Positions of location sensors with significant under-predictions in results predicted Phast CFD for FLADIS09 test case (values in the graph indicate ratios between predicted and observed concentrations at locations of the nearby dots)

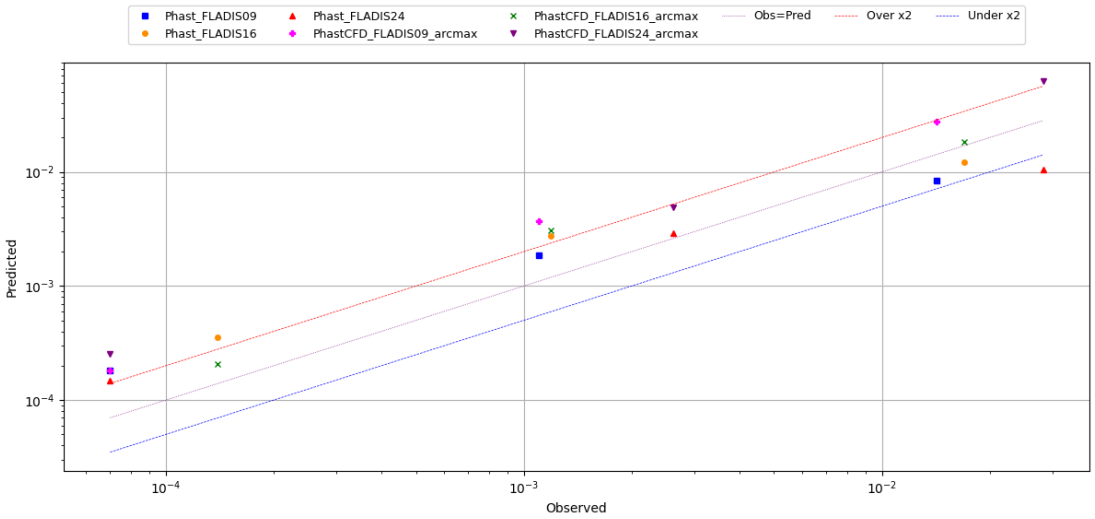

Figure 20 Comparing predictions of arcwise maximum concentration by Phast CFD, Phast and measurements for the FLADIS test cases

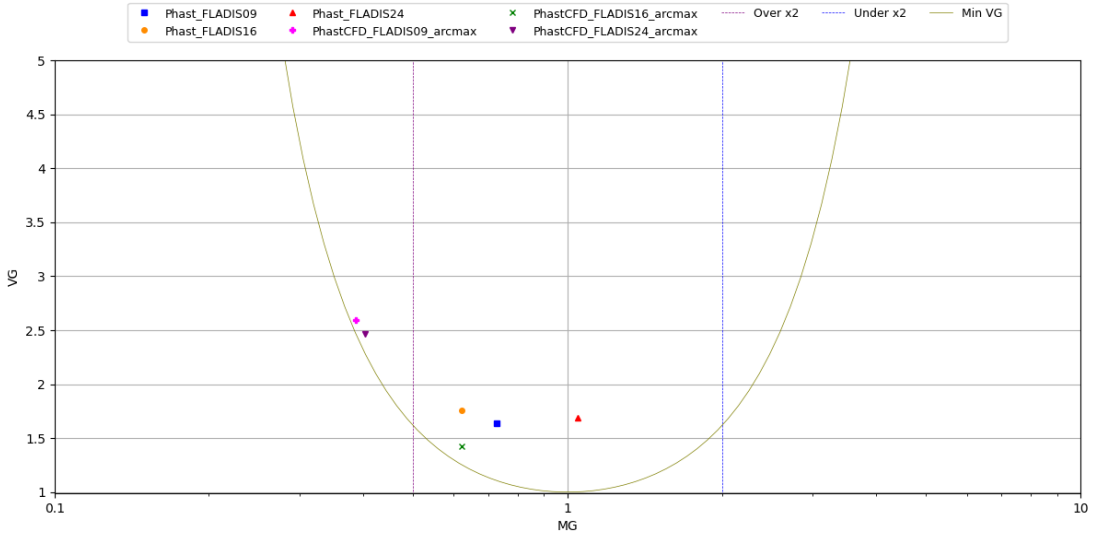

Figure 21 Statistical assessment of Phast CFD predictions of arcwise maximum concentration for the FLADIS test cases

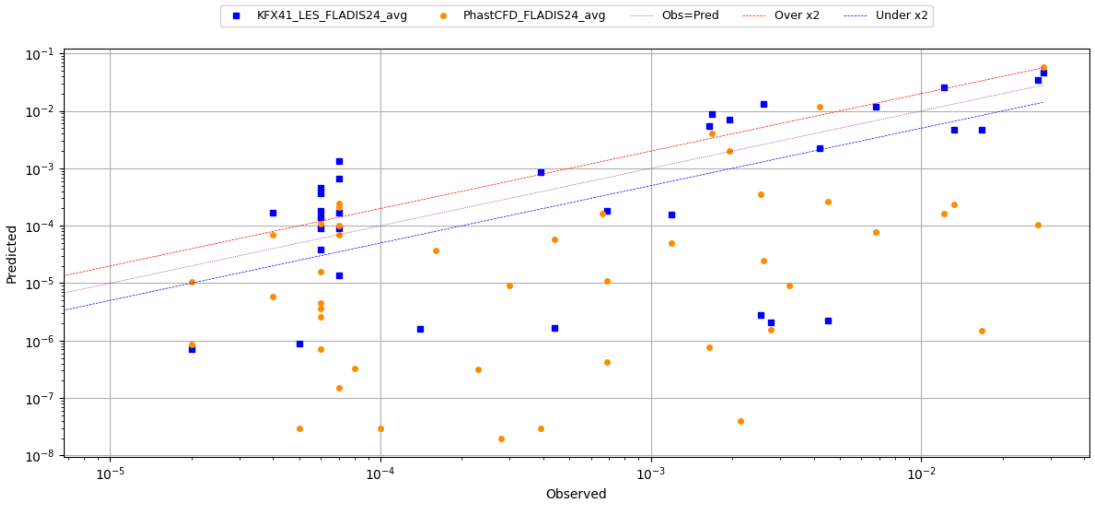

Figure 22 Comparing the results of Phast CFD and KFX LES against measurements for the FLADIS24 test case

4 RADIATION OF JET FIRES

4.1 Horizontal jet fires

4.1.1 The test cases

Seven tests (1042, 1040, 1083, 1037, 1033, 1036 and 1089) that relate to free jet flames by Johnson et al (Johnson A.D., 1994) were used to validate the Johnson Cone jet fire model implemented in Phast for horizontal vapour releases (DNV, Validation: Jet fire, 2023). Detailed information about these test cases can be found in the validation document of Phast for the jet fire models. In this analysis, three of the test cases were analysed to compare jet fire predictions between Phast and Phast CFD. The release and ambient conditions are listed in Table 4.

Table 4 Release and ambient conditions of the Johnson jet fire test cases

	1033	**1083**	**1089**
Material	Natural gas	Natural gas	Natural gas
Mass flowrate (kg/s)	8.2	8.6	3.7
Expanded temperature (K)	172.8	203.7	143.9
Expanded diameter (m)	0.119	0.1472	0.07279
Release height (m)	3	3	3
Hole size (mm)	75	152	20
Ambient air temperature (K)	282.35	281.25	285.85
Ambient air pressure (bar)	1	0.984	0.970
Ambient humidity (%)	81	80	91
Wind Speed (m/s)	4	0.3	9
Wind direction from north (°)	255	340	260
Pasquill stability	F	F	F
Surface roughness (mm)	183.156	183.156	183.156

4.1.2 Results and observations

- These test cases were integral to the data used to develop the Johnson Jet fire model implemented in Phast. It is unsurprising that Phast predictions are in good agreement with the measurements, as shown in Figure 23 & Figure 24. In this comparison, both measurements and Phast predictions are directional radiation, i.e. radiation measured by radiometers with fixed directions.
- Phast CFD predictions exhibit a conservative trend cross all three test cases, particularly Test-1083, as shown in Figure 25 & Figure 26. Phast CFD predicts maximum radiation at the measurement locations, i.e. radiation for point observers, and so the predictions should be slightly higher than the measurements which are for planer observers. Hence, a portion of the conservatism observed in Figure 25 & Figure 26 can be attributed to the difference in observer type in Phast CFD predictions and measurements.
- However, only a small portion of the conservatism shown in Figure 25 & Figure 26 are due to differences in observer type, as demonstrated in Figure 27 & Figure 28 for the Test-1033 case. Radiation variances between point and planer observers are small in Test-1033 and similar behaviors are also observed in other test cases. This indicates that radiometers were exposed to near maximum radiation at the fixed directions during the tests and the measured radiation are close to radiation of point observers. Thus, the measurements can be compared with Phast CFD predictions. KFX was required to obtain radiation of planer observers at specified directions.

- However, the majority of Phast CFD predictions fall within an acceptable range – specifically, within the factor-of-two lines. Therefore, the predictions are considered reasonable.

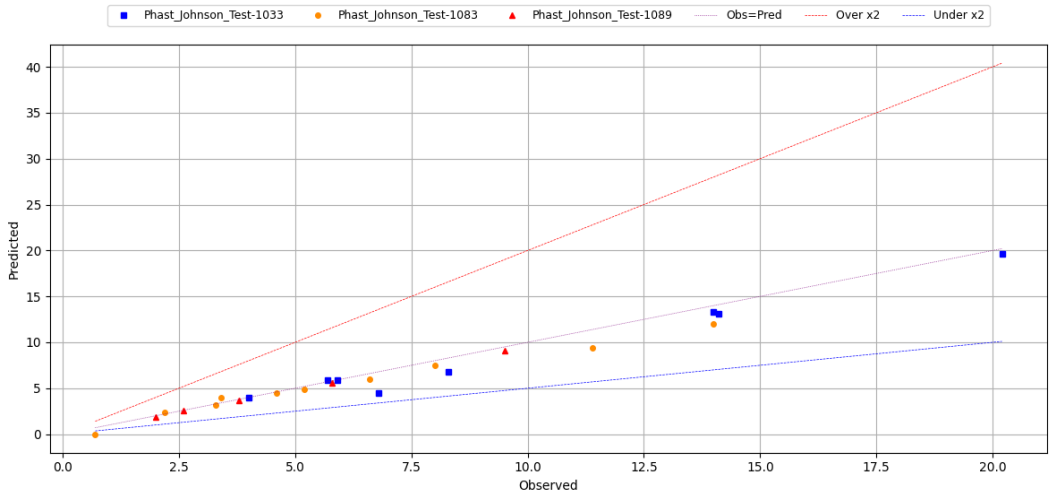

Figure 23 Comparing measured incident radiation (kW/m^2) against Phast predictions for the Johnson jet fire test cases

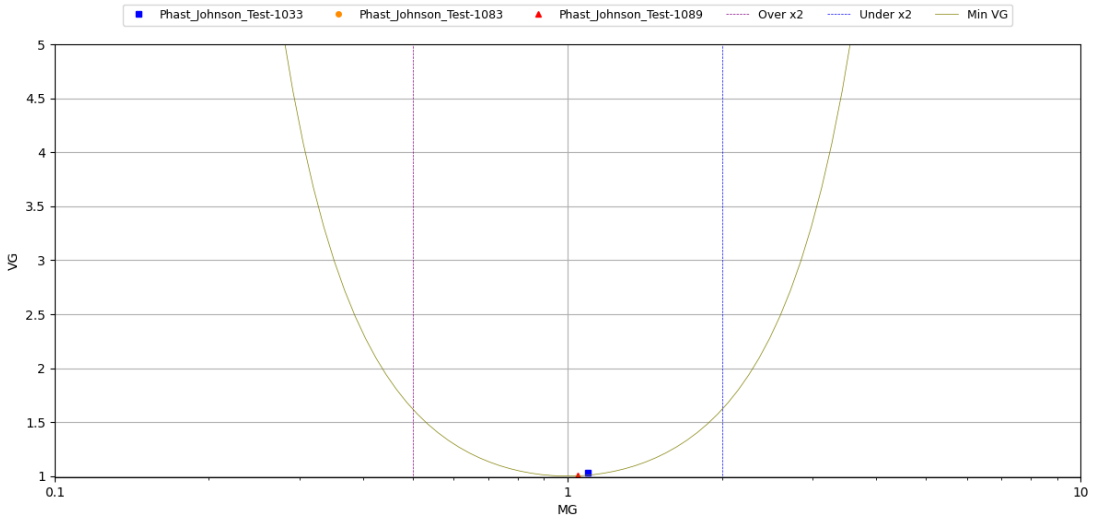

Figure 24 Statistical assessment of Phast predictions of incident radiation for the Johnson jet fire test cases

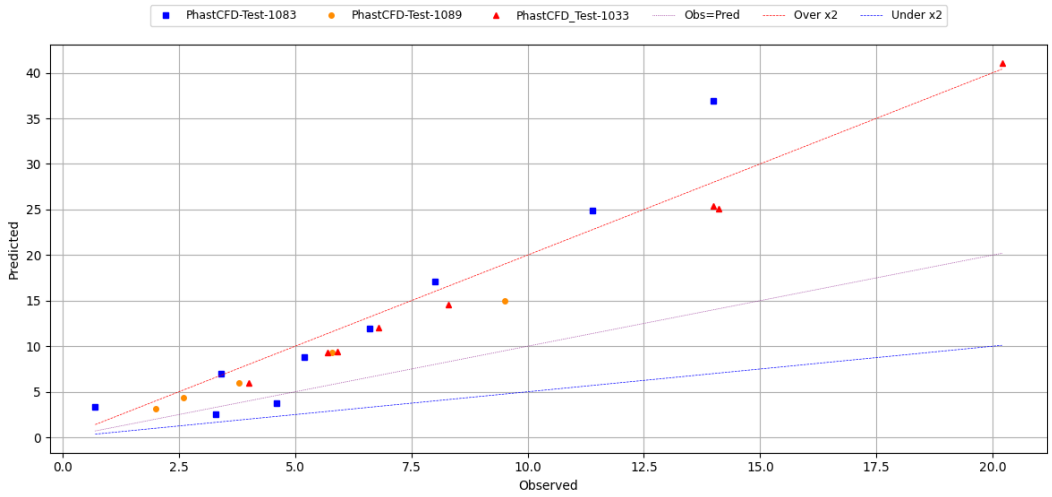

Figure 25 Comparing measured incident radiation (kW/m^2) against Phast CFD predictions for the Johnson jet fire test cases

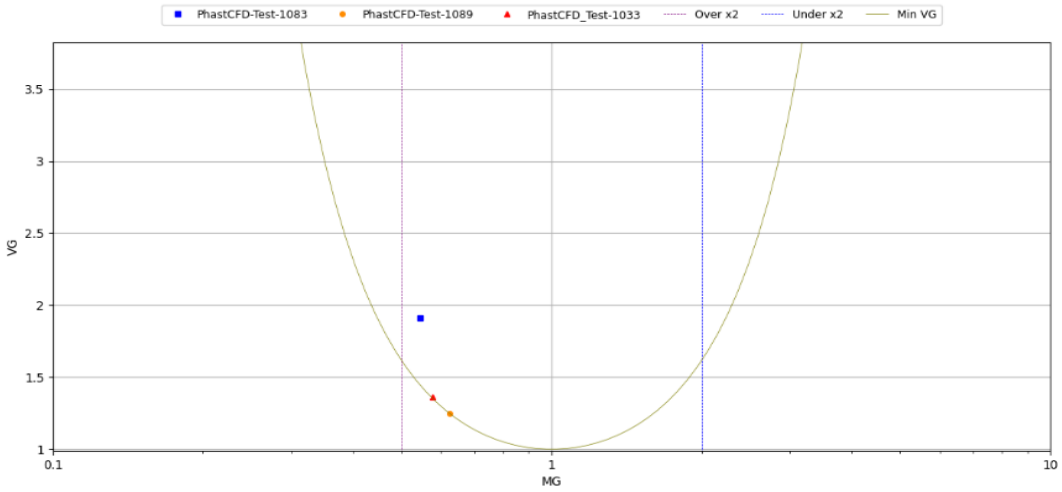

Figure 26 Statistical assessment of Phast CFD predictions of incident radiation for the Johnson jet fire test cases

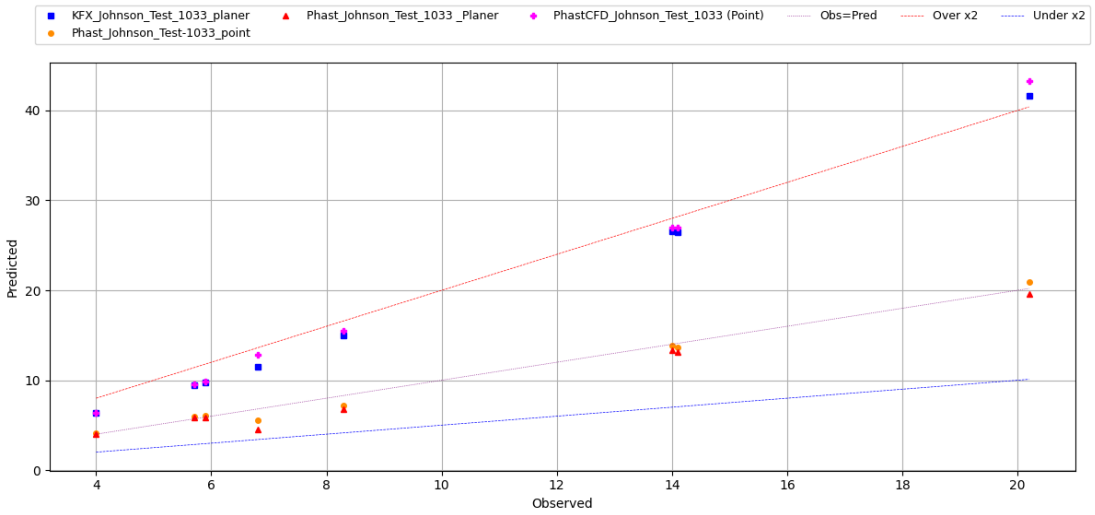

Figure 27 Comparing predictions of incident radiation by Phast, Phast CFD and KFX with point and planer observer types (kW/m^2) for the Johnson 1033 test case (point means point observer type, planer means planer observer type)

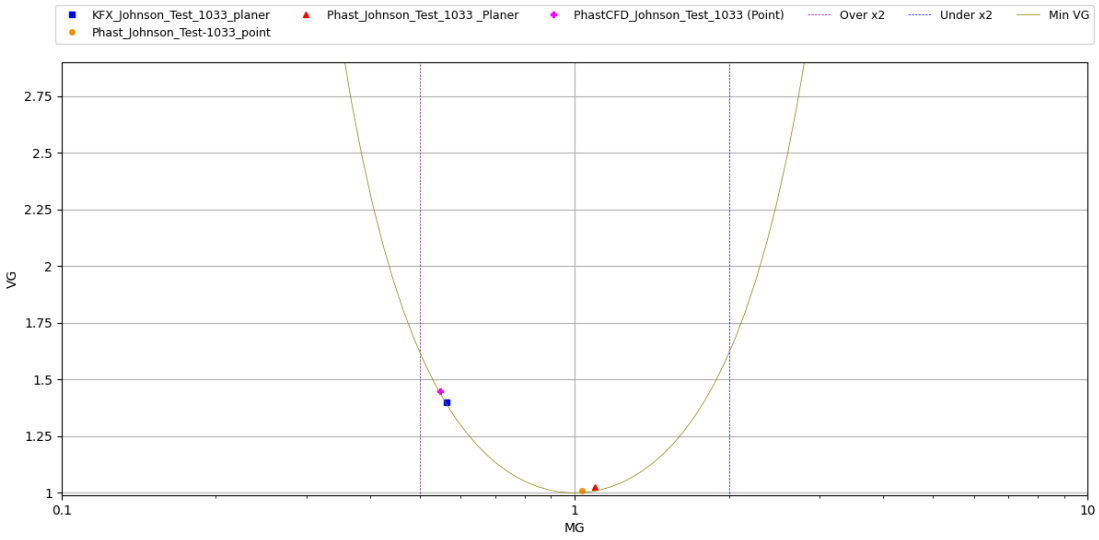

Figure 28 Statistical assessment of predictions of incident radiation by Phast, Phast CFD and KFX with point and planer observer types for the Johnson 1033 test case (point means point observer type, planer means planer observer type)

4.2 Vertical jet fires

4.2.1 Input data

The Chamberlain Cone jet fire model in Phast was validated against field data reported by Chamberlain (Chamberlain, 1987). This model requires specification of the fuel's post-expansion thermodynamic properties (temperature or liquid fraction) and dynamic properties (expanded radius or velocity) as input data. Unfortunately, the values for these release properties were not included in the report. To address this, back calculations were performed using secondary data and recommended discharge equations. As a result, the post-expansion temperature and velocity for each test case were estimated, as listed in the table below.

Table 5 Release and ambient conditions for Chamberlain test cases

	Test 3A	**Test 3D**	**Test 4A**	**Test 4C**
Material	Natural gas	Natural gas	Natural gas	Natural gas
Mass flowrate (kg/s)	21.1	55.6	5.6	22.2
Expanded temperature (K)	289.83	326.51	284.15	198.3
Jet velocity (m/s)	26.83	74.29	238.71	544.83
Release height (m)	110	110	10	10
Ambient air temperature (K)	289.15	286.15	289.45	187.45
Ambient air pressure (bar)	1	1	1	1
Ambient humidity (%)	53	56	50	51
Wind Speed (m/s)	7.5	8	8.1	10.3
Pasquill stability	D	D	D	D

4.2.2 Results and observations

- These test cases were integral to the dataset used to develop the Chamberlain Jet fire model implemented in Phast. Consequently, Phast predictions are in good agreement with the measurements, as shown in Figure 29 Figure 29 & Figure 30.
- Radiation values compared here are for point observers in Test 3A & 3D. Measured radiation in Test 4A & 4C is for planer observers (i.e. radiation measured by radiometers with fixed directions). However, the radiometers in Test 4A & 4C were exposed to near maximum radiation during the tests as demonstrated in Figure 31. Thus, the measured radiation is close to radiation of point observers and can be compared with Phast CFD predictions.
- Overall, Phast CFD predictions are satisfactory. All predictions for the four test cases fall within the factor-of-two lines, as shown in Figure 32 & Figure 33. Minor variations are observed in case Test 3A.

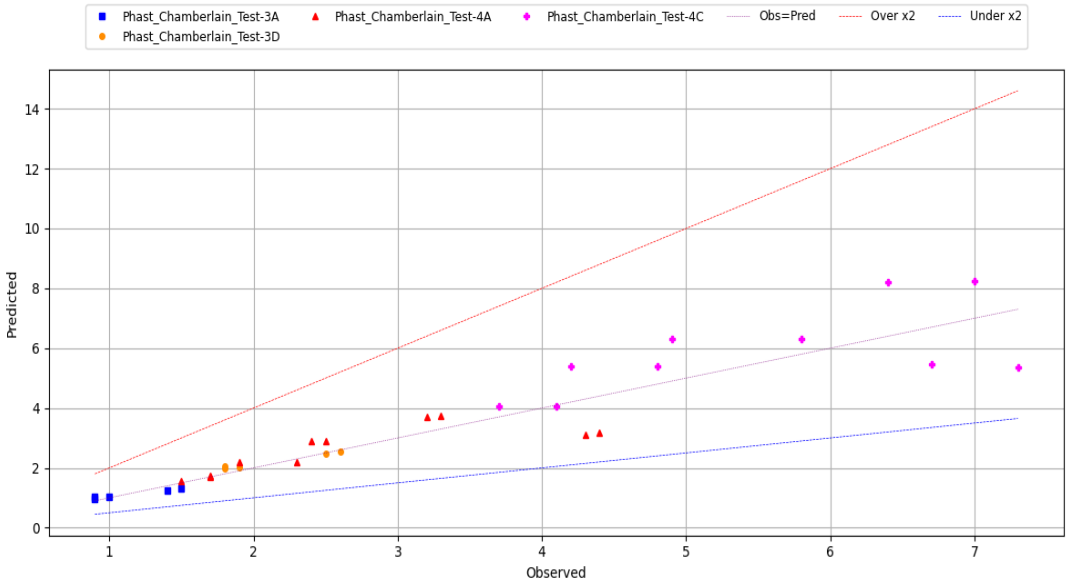

Figure 29 Comparing measured incident radiation (kW/m^2) against Phast predictions for the Chamberlain test cases

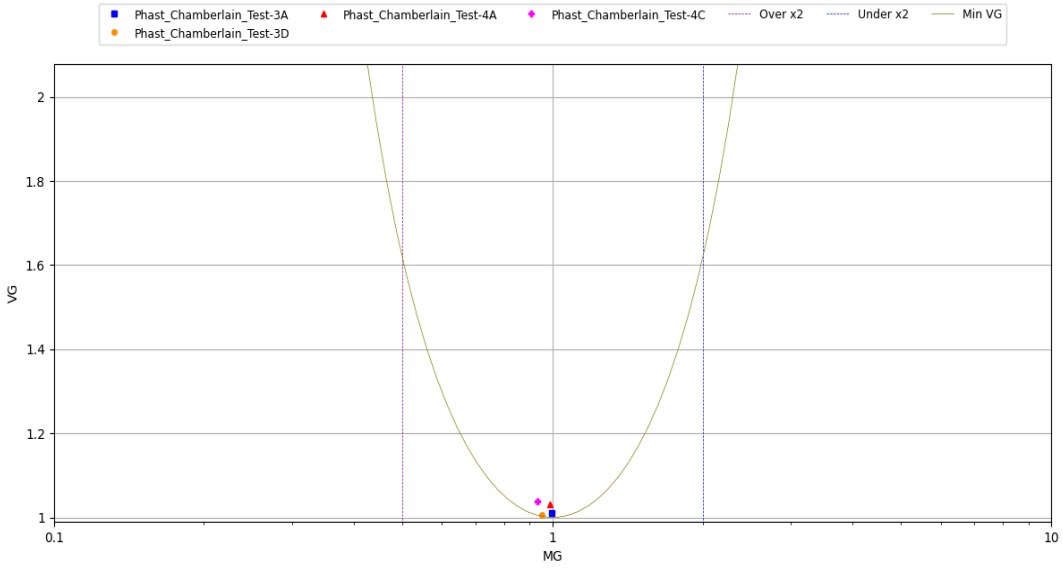

Figure 30 Statistical assessment of Phast predictions of incident radiation for the Chamberlain test cases

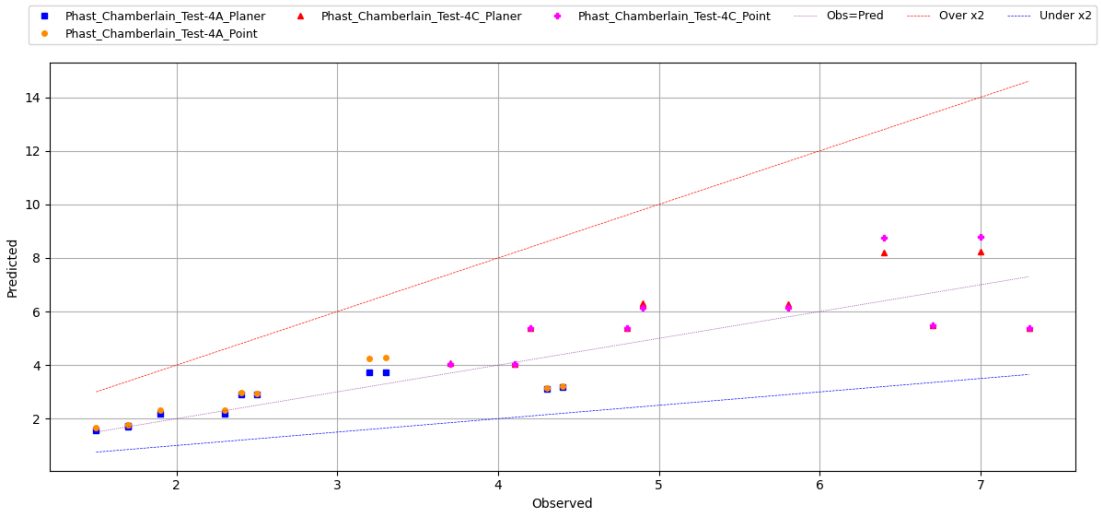

Figure 31 Comparing predictions of incident radiation by Phast with point and planer observer types (kW/m^2) for the Chamberlain test case (point means point observer type, planer means planer observer type)

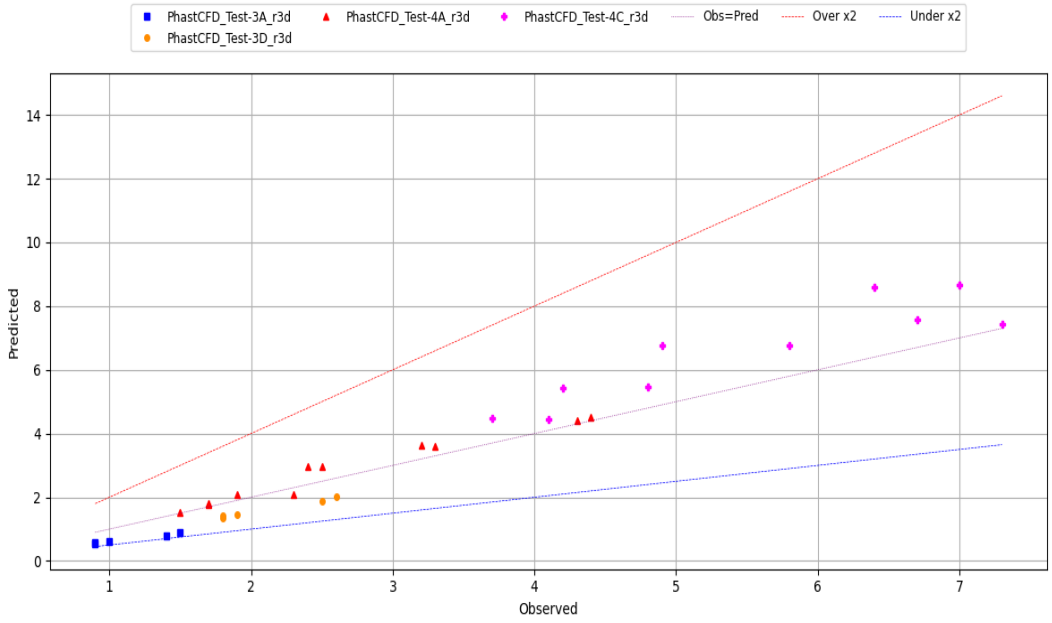

Figure 32 Comparing measured incident radiation (kW/m^2) against Phast CFD predictions for the Chamberlain test cases

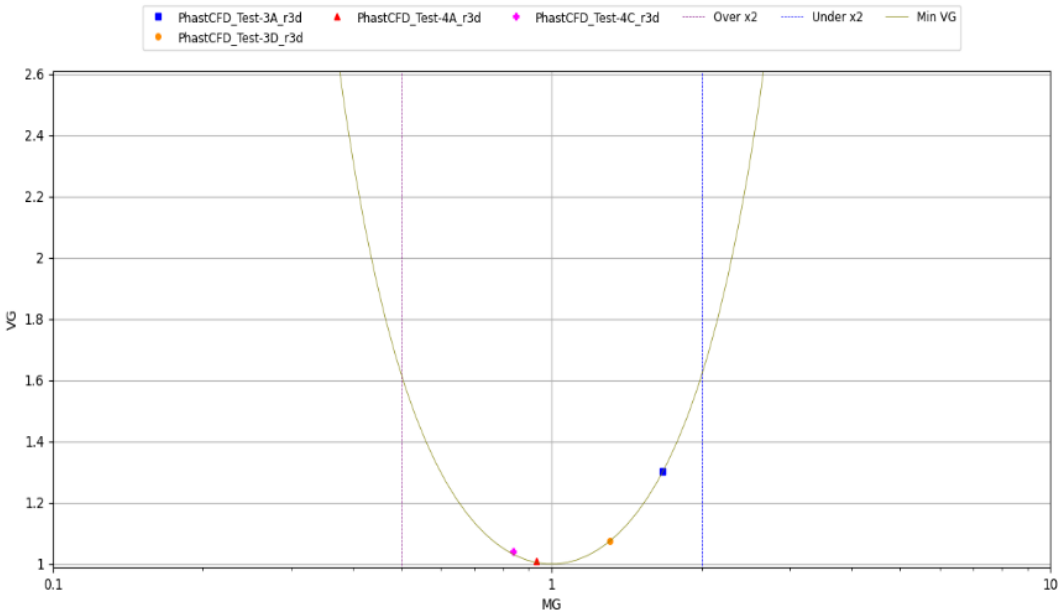

Figure 33 Statistic assessment of Phast CFD predictions of incident radiation for the Chamberlain test cases

4.3 Horizontal two-phase jet fires

4.3.1 Test cases

Phast CFD predictions for horizontal two-phase jet fires are assessed against radiation measurements from three test cases conducted by Bennet et al (Bennett, 1991). These same cases were also used to validate the Cook Cone model in Phast for two-phase jet fires. Table 6 below lists the input data required for these cases as for the standalone jet fires in Phast. Some of the input data were back-calculated, and additional details can be found the theory manual of the jet fire models of Phast (DNV, Jet fire, 2023).

Table 6 Release & ambient conditions of the Cook model

	Bennett 3006	**Bennett 3026**	**Bennett 3029**
Material	Propane	Propane	Propane
Mass flowrate (kg/s)	1.5464	16.1	18
Post expansion liquid fraction	0.737411	0.758563	0.77005
Jet velocity (m/s)	168.129	152.71	145.67
Release height (m)	1.5	3	1.5
Ambient air temperature (K)	286.35	286.85	281.15
Ambient air pressure (bar)	1	1	1
Ambient humidity (%)	79	59	82
Wind Speed (m/s)	5.8	3.7	2
Pasquill stability	D	D	D
Surface roughness (mm)	183.156	183.156	183.156

4.3.2 Results and observations

- All radiation values compared here for two-phase releases are for point observers.
- Most Phast predictions fall within the factor-of-two lines, except for two measurements in the Bennett 3006 test case, as shown in Figure 34. Overall, Phast has produced slight overpredictions, as indicated by the statistical assessment shown in Figure 35.
- Phast CFD predictions are generally satisfactory, with the majority of predictions falling within the factor-of-two lines. However, there is one measurement in the Bennett 3006 case and two measurements in the Bennett 3029 case that deviate, as shown in Figure 36. The predictions are conservative in all three cases, particularly for the Bennett 3029 case.

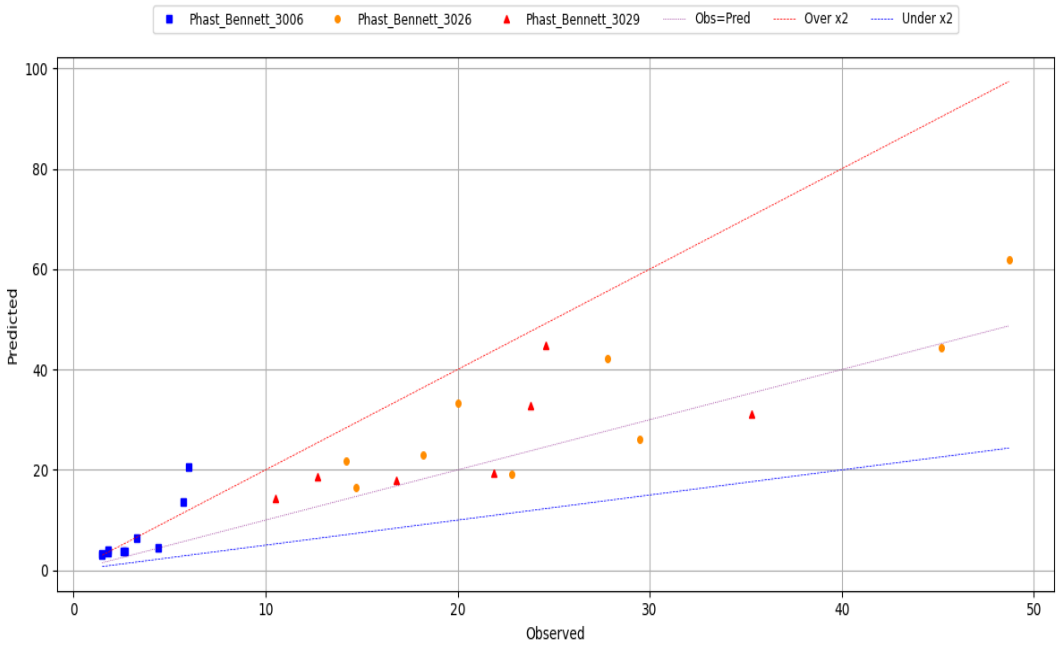

Figure 34 Comparing measured incident radiation (kW/m^2) against Phast predictions for the Bennett test cases of two-phase jet fires

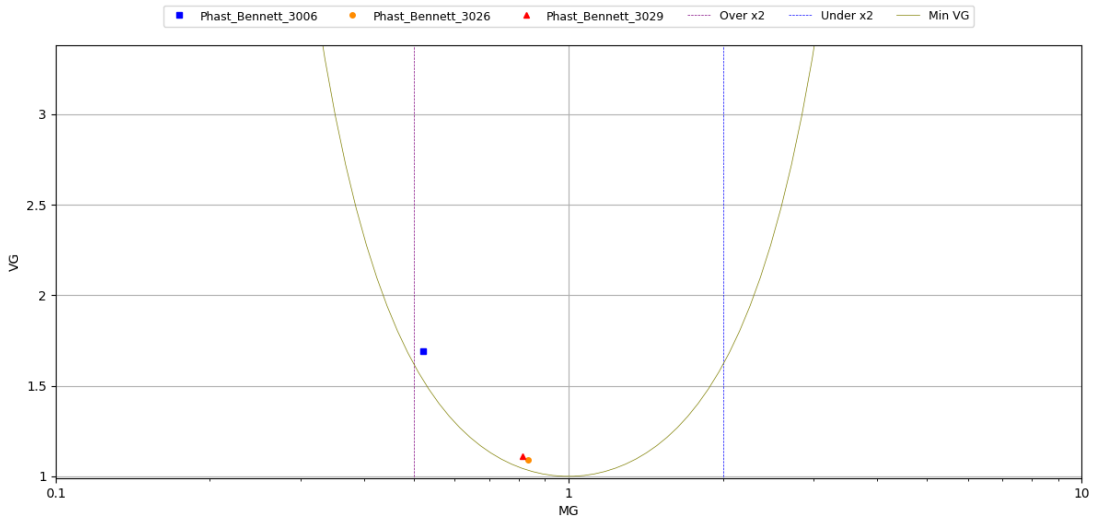

Figure 35 Statistical assessment of Phast predictions of incident radiation for the Bennett test cases of two-phase jet fires

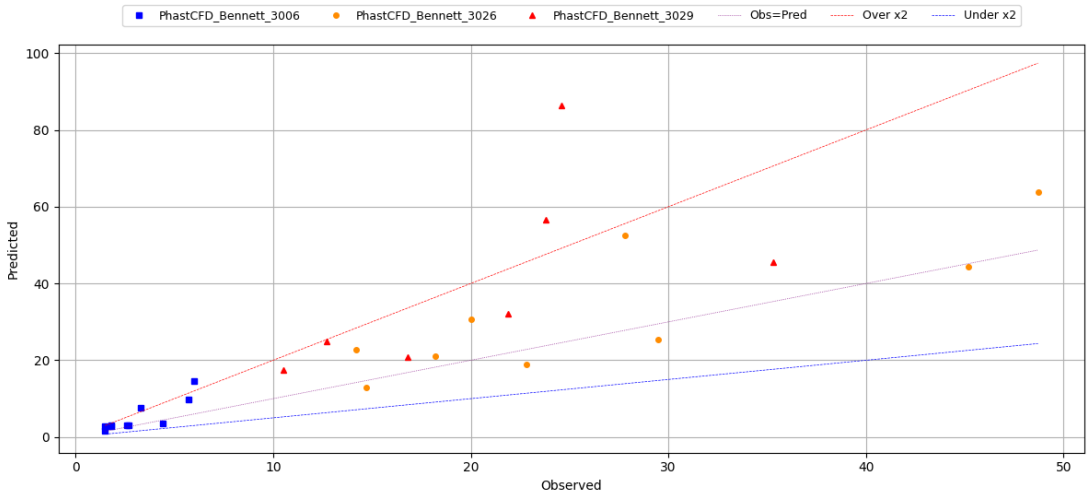

Figure 36 Comparing measured incident radiation (kW/m^2) against Phast CFD predictions for the Bennett test cases of 2-phase jet fires

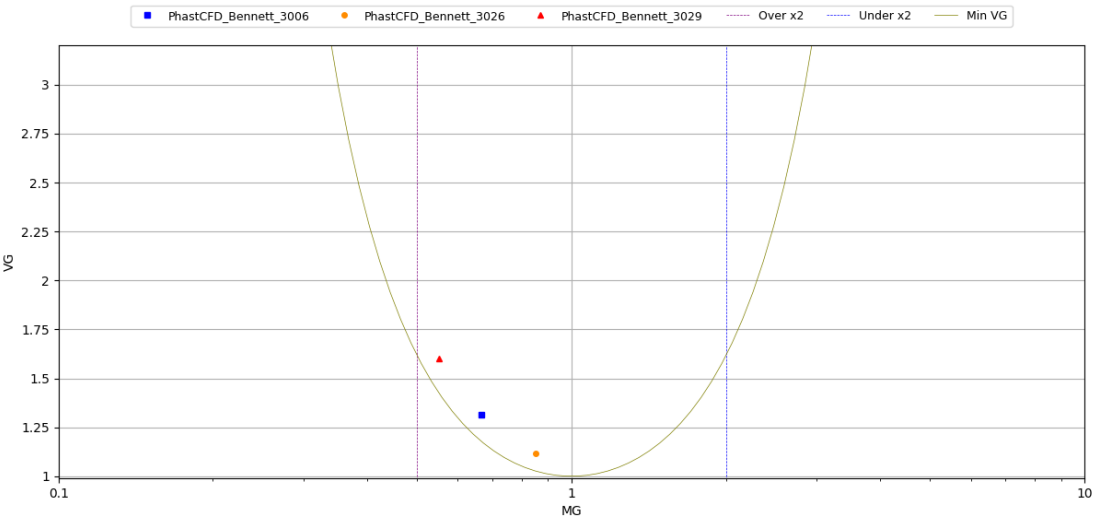

Figure 37 Statistical assessment of Phast CFD predictions of incident radiation for the Bennett test cases of two-phase jet fires

4.4 Hydrogen jet fires

4.4.1 The test cases

Tests of hydrogen jet fires were conducted by DNV at the Spadeadam test site on behalf of Air Products & Chemicals Inc. in 2009 (Advantica, 2009). These tests were also used to develop the Miller jet fire model for hydrogen releases, which was implemented in Phast 8.6. Table 7 below lists the input data in the Phast studies for the test cases.

Table 7 Release and ambient conditions of the test cases for hydrogen test cases

	13_AP&DNVGL	14_AP&DNVGL	15_AP&DNVGL
Material	Hydrogen	Hydrogen	Hydrogen
Mass flowrate (kg/s)	1	7.5	6.6
Expanded temperature (K)	142.303	141.385	142.065
Jet velocity (m/s)	1969.52	1978.97	1971.90
Orifice diameter (mm)	20.9	52.5	20.9
Release height (m)	3.25	3.25	3.25
Ambient air temperature (K)	280	287	287
Ambient air pressure (bar)	1	1	1
Ambient humidity (%)	94.3	94.2	94.3
Wind Speed (m/s)	3.4	2.6	2.6
Pasquill stability	D	D	D
wind direction relating the release direction (°)	178.5	-151.7	-142.7
Surface roughness (mm)	183.156	183.156	183.156

4.4.2 Results and observations

- All radiation values compared here for hydrogen jet fires are for point observers
- Most Phast CFD predictions fall within the factor-of-two lines, except for one measurement in the 14_AP_DNVGL and 15_AP_DNVGL test cases, as shown in Figure 38.
- Minor variations are observed in these test cases, as shown in Figure 39 from the statistical assessment.
- Overall, Phast CFD predictions for hydrogen jet fires are satisfactory.

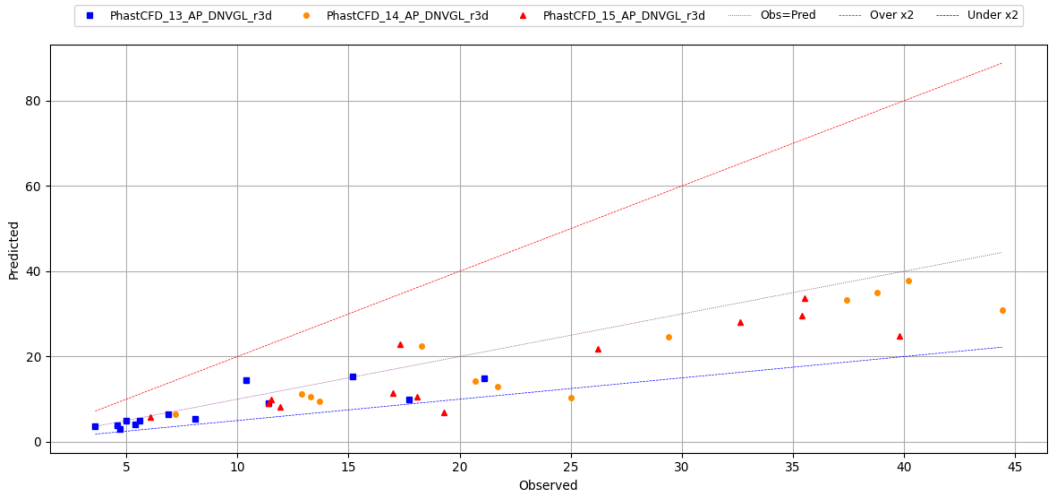

Figure 38 Comparing measured incident radiation (kW/m^2) against Phast CFD predictions of hydrogen jet fires

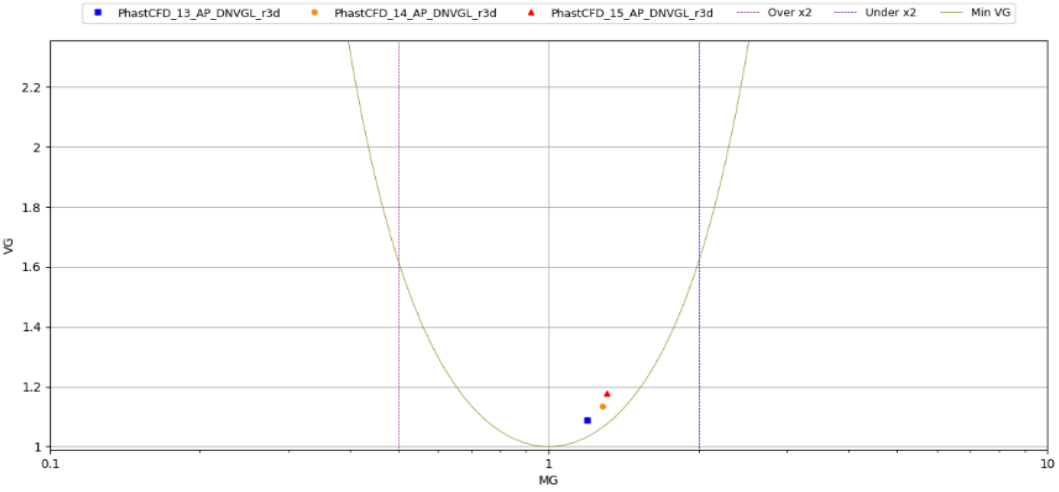

Figure 39 Statistical assessment of Phast CFD predictions of incident radiation for hydrogen jet fires

4.5 Jet fire with a large release area

4.5.1 Test case

This test case involves a hydrogen jet fire for the development the Miller jet fire model (Fishburne, 1979). Table 8 provides the input data used in the Phast study for this specific case. It is worth noting that the expanded diameter for this case is 1.4415 meters, which is relatively large compared to most other test cases. The significance of this lies in the fact that the expanded diameter of the input determines the size of the release cell employed in Phast CFD simulations. Therefore, this case has been specifically examined to evaluate the impact of the release area on the predicted results.

Table 8 Release and ambient conditions for the Fishburne test

	Value
Material	Hydrogen
Mass flowrate (kg/s)	22
Release temperature (deg C)	0
Release velocity (m/s)	150
Release height (m)	127
Ambient air temperature (deg C)	9.85
Ambient air pressure (bar)	1
Ambient humidity (%)	58
Wind Speed (m/s)	1.5
Pasquill stability	C/D
Surface roughness (mm)	183.156

4.5.2 Results and observations

- There is no radiation measurement available for this case. Therefore, Phast CFD results are only compared with KFX predictions for the same release with refined grids at the release point.
- Notable differences between the two sets of results can be observed in Figure 40 & Figure 41 for radiation distribution. KFX results, obtained with refined release cells, show higher radiation distances, i.e. larger contours for the specified radiation intensities. The differences are likely to be caused by the large release cells automatically generated in the Phast CFD simulations.
- Therefore, for scenarios with large release areas, Phast CFD may produce under-predictions of the radiation extent. Users are advised to simulate such cases using KFX with finer grid resolutions at the release point.

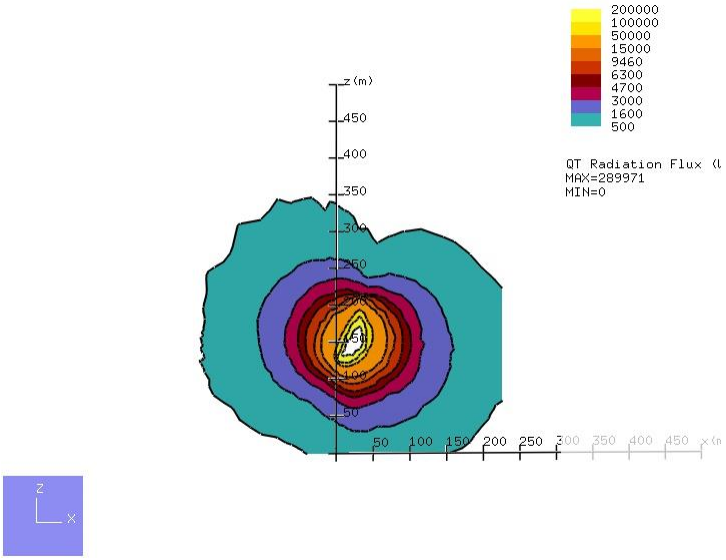

Figure 40 Phast CFD prediction of radiation distribution (kW/m^2) on a vertical plane (displayed using KFX View)

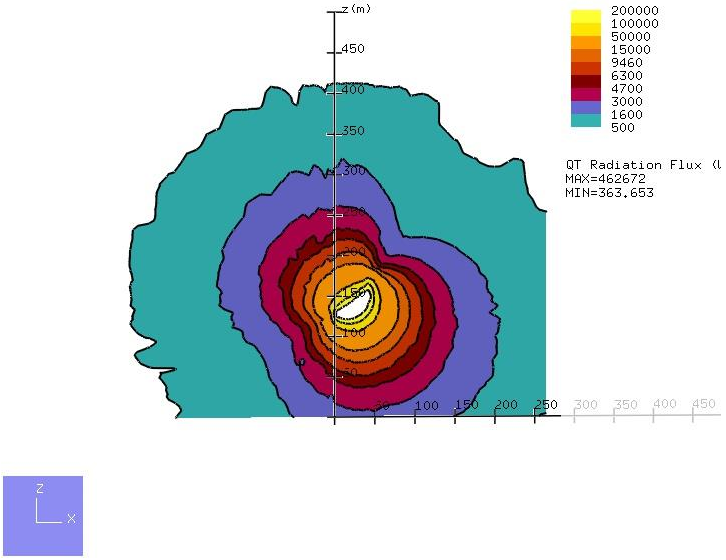

Figure 41 KFX prediction with the same input data and refined grid as Phast CFD on the same vertical plane as shown above

4.6 Summary of Jet fire simulations

- Phast CFD predictions for jet fires are generally satisfactory based on the results of the test cases shown above.
- For scenarios with large release areas, Phast CFD may produce under-predictions of the radiation extent.

5 RADIATION OF POOL FIRES

5.1 Test cases

Johnson conducted three tests related to LNG pool flames with diameters of 1.8, 6.1, and 10.6 metres (i.e. Field Trials 1, 6 and 7, respectively) (Johnson, 1992). These tests were carried out in shallow bunds with thermally insulated concrete floors to minimise heat transfer to the pool from the substrate. Detailed information about the validation process can be found in the theory manual for the pool fire models implemented in Phast (DNV, Pool fire model, 2023). Table 9 below shows the input data for the test cases.

Table 9 Pool and ambient conditions of the Johnson field trials

	Field trial1	**Field trial 6**	**Field trial 7**
Material	LNG	LNG	LNG
Pool diameter (m)	1.8	6.1	10.6
Air temperature (K)	283.15 (assumed)	280.15	284.25
Air pressure (bar)	1.01325(assumed)	0.943	0.943
Relative Humidity (%)	70(assumed)	83	87
Wind speed (m/s)	2.4	6.6	4.0
Wind direction (clockwise from North)	270	250	90

5.2 Results & observations

- Phast CFD predictions of pool fires are sensitive to ground roughness, as shown in Figure 42. Surface roughness of 5mm was used for the results shown below.
- The majority of Phast CFD predictions for the three test cases are within the factor-of-two lines, as shown below in Figure 43. Overall, the predictions are satisfactory.
- However, the Phast CFD predictions are less conservative at some locations (i.e. the predictions are below the factor-of-two lines), as shown in Figure 43 & Figure 44. Pool fires have low momentum and are easily disturbed by wind variations, such as fluctuations in wind speed and direction, or effects of the local terrain and obstructions. These variations are not included in the Phast CFD simulations and may have contributed to the under-predictions.

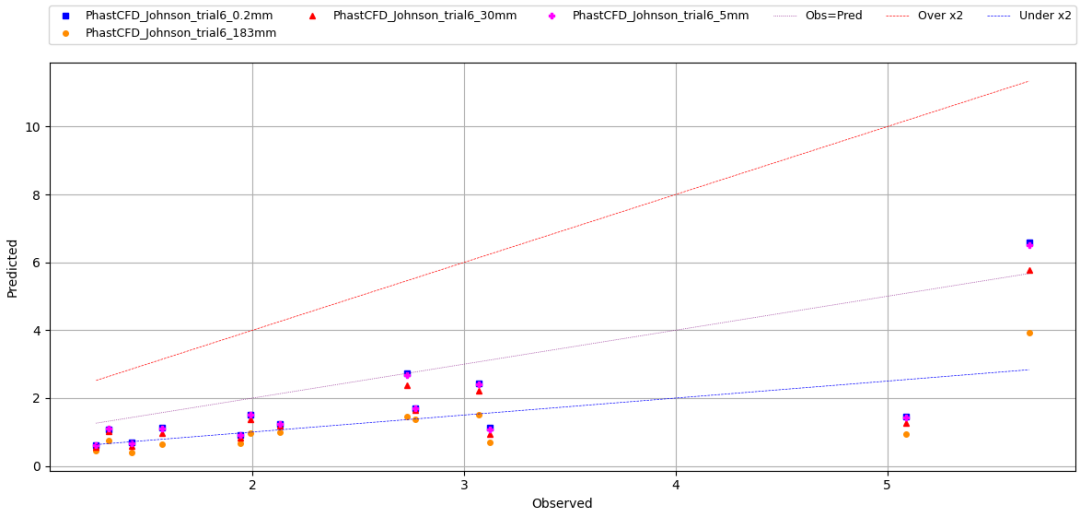

Figure 42 Sensitivity analysis of Phast CFD predictions of incident radiation (kW/m^2) with ground roughness for pool fire simulations

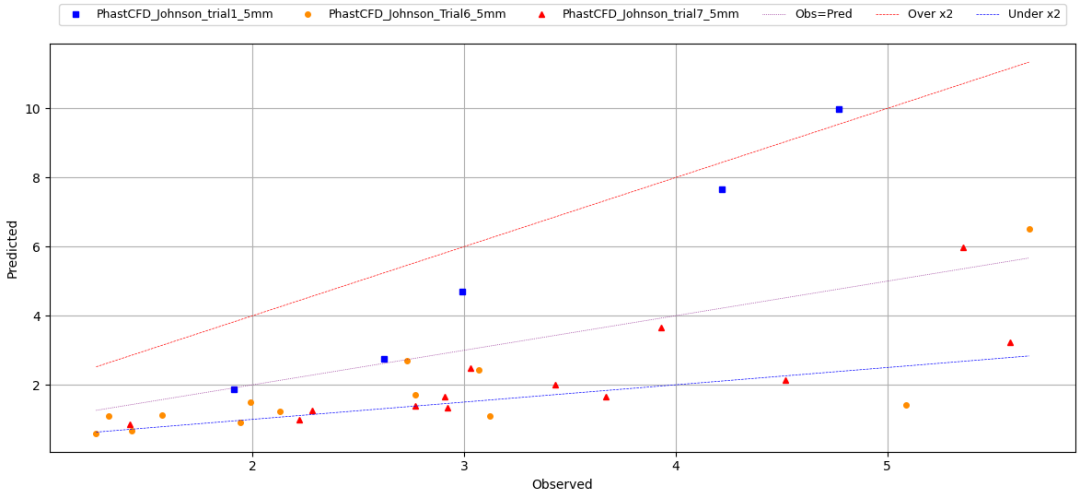

Figure 43 Comparing measured incident radiation(kW/m^2) against Phast CFD predictions of the Johnson trials of LNG pool fires

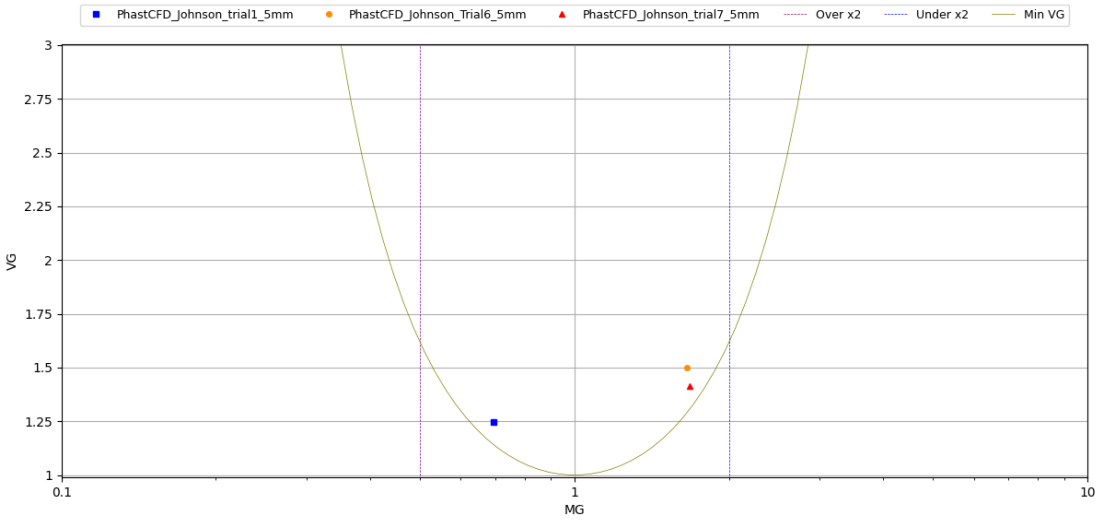

Figure 44 Statistical assessment of Phast CFD predictions of incident radiation for Johnson trials of LNG pool fires

6 CONCLUSIONS AND RECOMMENDATIONS

The results from Phast CFD have been compared with predictions from Phast and measurements across a range of test cases of dispersion, jet fires and pool fires. The key findings are as follows:

- **Dispersion predictions:** Phast CFD predictions of dispersion for vapor releases are satisfactory. However, the predictions are sensitive to surface roughness. Thus, appropriate surface roughness values are important for releases near the ground, instead of relying on the default setting of Phast.
- **Two-phase ammonia test cases:** In the case of the two-phase ammonia test cases, Phast CFD tends to produce under-predictions for dispersion. While the predictions follow a similar trend as Phast, they exhibit broader scattering. However Phast CFD does slightly overpredict arcwise maximum concentrations for all FLADIS test cases. This behaviour of Phast CFD predictions can be primarily attributed to the fact that Phast CFD results are predicted with fixed wind directions, which does not account for fluctuations in ambient conditions, such as wind meandering. Additionally, droplet characteristics, including droplet size distribution and spray angle, may have also contributed to the observed discrepancies. So, for scenarios with stable ambient conditions or scenarios with fixed directions in risk assessments, Phast CFD should give good dispersion results. However, for cases with large variations in ambient conditions, Phast CFD simulations for multiple wind speeds and directions may be necessary to achieve a comprehensive dispersion result. Users with access to the KFX software can use the KFX Large Eddy Simulation (LES) model to get more accurate dispersion results.
- **Jet fire predictions**: While predictions of jet fires by Phast CFD are satisfactory, potential under-predictions are observed for jet fire scenarios with large release areas, i.e. scenarios with large, expanded diameters.
- **Pool fire predictions**: Predictions of pool fires by Phast CFD are also satisfactory. The results are sensitive to surface roughness; therefore, appropriate surface roughness is essential, rather than relying on the default setting of Phast

It is important to note that the test cases analysed in this work did not include complex geometries, as these cases often can be effectively solved by the simple models implemented in Phast. Nevertheless, for scenarios with complex geometries or requiring detailed results, both Phast CFD and KFX offer superior capabilities.

7 REFERENCES

Advantica. (2009). *Report on hydrogen jet fires carried out on behalf of Air Products & Chemicals Inc.* Private report.

Allason, D. (2009). Report on hydrogen jet fires carried out on behalf of Air Products & Chemical Inc. . *Report No 8653*.

Bennett, J. C. (1991). *Large scale narural gas and LPG jet fires.* TNER 91.022.

Chamberlain, G. A. (1987). Development in design methods for predicting thermal radiation frlm flares. *Chem. Eng. Res. Des.*, Vol 65, pp299-309.

DNV. (2023). Jet fire. *Phast theory Manual*.

DNV. (2023). *Pool fire model.*

DNV. (2023). *Validation: Jet fire.*

DNV. (2023). *Validation: Unified Dispersion Model.*

Fishburne, E. a. (1979). The dynamics and radiant intensity of large hydrogen flame. *Colloquium on Fire and Explosion*.

Johnson A.D., B. H. (1994). A model for predicting the thermal radiation hazard from large scale horizontally released natural gas jet fires. *Trans IChemE*, Vol 72, Part B, pp 157-166.

Johnson, A. (1992). A model for predicting thermal radiation hazards from large-scale LNG pool fires. *IChemE Symp.*, Series 130, pp 507-524.

Nielsen, M. O. (1996). *FLADIS field experiments.* Roskilde, Denmark: Final report Tiso-R-898(EN), Riso National Laboratory.

Roberts, P. S. (2006). Dispersion of hydrogen from high-pressure sources. *Institution of Chemical Engineers Symposium Series 151*, (pp. 410-421).